International Journal of Scientific Engineering and Applied Science (IJSEAS) – Volume-3, Issue-4, April 2017
ISSN: 2395-3470
www.ijseas.com

The Relationships between the Bosonic Standing Waves and the Fermionic Traveling Waves

Takashi Kato
Institute for Innovative Science and Technology, Graduate School of Engineering, Nagasaki Institute of Applied Science, 3-1, Shuku-machi, Nagasaki 851-0121, Japan
E-Mail: KATO_Takashi@NiAS.ac.jp

Abstract

In the Meissner effect, the electric and magnetic fields can be induced because the initial ground electronic state tries not to receive the applied external magnetic field, as much as possible, in order that the electronic state does not change from the initial ground electronic state. This expulsion originates from very stable bosonic standing wave state (70 eV) with zero momentum formed by two components of the traveling waves of two fermionic electrons with opposite momentum and spins. In the closed-shell electronic structure in superconductivity, two electrons occupying the same orbital have the opposite momentum and spins by each other, and are condensated into the zero-momentum state (Bose–Einstein condensation), and therefore, there is standing wave with zero momentum formed by two electrons. Related to the relationships between the bosonic standing waves and fermionic traveling waves, we also discuss the relationships between the entropy and the time.

Keywords: *Meissner Effect; Bose–Einstein Condensation; Fermionic Traveling Waves; Bosonic Standing Waves.*

1. Introduction

The effect of vibronic interactions and electron–phonon interactions [1–7] in molecules and crystals is an important topic of discussion in modern chemistry and physics. The vibronic and electron–phonon interactions play an essential role in various research fields such as the decision of molecular structures, Jahn–Teller effects, Peierls distortions, spectroscopy, electrical conductivity, and superconductivity. We have investigated the electron–phonon interactions in various charged molecular crystals for more than 15 years [1–8]. In particular, in 2002, we predicted the occurrence of superconductivity as a consequence of vibronic interactions in the negatively charged picene, phenanthrene, and coronene [8]. Recently, it was reported that these trianionic molecular crystals exhibit superconductivity [9].

Related to the research of superconductivity as described above, in the recent research [10,11], we explained the mechanism of the Ampère's law (experimental rule discovered in 1820) and the Faraday's law (experimental rule discovered in 1831) in normal metallic and superconducting states [12], on the basis of the theory suggested in our previous researches [1–7]. Furthermore, we discussed how the left-handed helicity magnetic field can be induced when the negatively charged particles such as electrons move [13]. That is, we discussed the relationships between the electric and magnetic fields [13]. Furthermore, by comparing the electric charge with the spin magnetic moment and mass, we suggested the origin of the electric charge in a particle. Furthermore, in the previous research, we discussed the origin of the gravity, by comparing the gravity with the electric and magnetic forces. Furthermore, we showed the reason why the gravity is much smaller than the electric and magnetic forces [14]. We discussed the origin of the strong forces, by comparing the strong force with the gravitational, electric, magnetic, and electromagnetic forces. We also discussed the essential properties of the gluon and color charges, and discussed the reason why the quarks and gluons are confined in hadron [15]. Furthermore, we discussed the origin of the weak forces, and discussed the reason why the parity violation can be observed in the weak interactions [16]. We also suggested the relationships between the Cooper pairs in superconductivity and the Higgs boson in the vacuum [16,17]. Recently, we discussed the origin of the spin magnetic dipole moment, massive charge, electric monopole charge, and color charge for the particle and antiparticles at the particles and antiparticle spacetime axes, by considering that particles (antiparticles) can be formed by mixture of the wavefunction of more dominant particle (antiparticle) component and of less dominant antiparticle (particle) component [18]. We suggested the new interpretation of the spacetime axis in the special relativity [19]. We also discussed the mechanism of the particle–antiparticle pair annihilation in view of the special relativity [19].

In this research, we will suggest the relationships between the superconducting, normal metallic, and insulating states. Related to these relationships, in particular, related to the relationships between the bosonic standing waves and the fermionic traveling waves, and

between the non-equilibrium states and the equilibrium states, we will also discuss the relationships between the entropy and the time.

2. Relationships between the London Theory and the BCS Theory

Historically, the conventional BCS theory for superconductivity has been established by Bardeen, Cooper, and Schrieffer in 1957 on the basis of the phenomenological London theory established by London brothers in 1935, as follows. In 1935, London brothers explained the nondissipative diamagnetic currents in the closed-shell electronic structures with large energy gaps between the occupied and unoccupied orbitals in small materials such as He atoms and benzene molecules (Scheme 1). They suggested that under the applied magnetic field, the atomic and molecular orbitals in He atoms and benzene molecules are very rigid, and thus if we assume that the canonical momentum $\boldsymbol{p}_{\text{canonical}}$ value, which denotes the total intrinsic momentum of each electron continues to become zero even under the applied magnetic field, and the $\boldsymbol{p}_{\text{em}}\left(=m_{\text{e}}\boldsymbol{v}_{\text{em}}\right)$ value, which denotes the momentum as a consequence of the electromotive forces, increases according to the applied magnetic field, the nondissipative diamagnetic currents in small materials such as He atoms and benzene molecules can be explained (Scheme 1). Furthermore, they suggested that superconductivity in the macroscopic sized solids can also be explained if we apply the London theory to the macroscopic sized superconductivity. The problem was to elucidate the mechanism how the stable electronic states with $\boldsymbol{p}_{\text{canonical}}=0$ can be realized. On the basis of the London theory, Bardeen, Cooper, and Schrieffer explained the mechanism of the realization of the electronic structures with $\boldsymbol{p}_{\text{canonical}}=0$ by considering that such stable electronic structures can be realized by electron pairing formed by two electrons with opposite momentum and spins as a consequence of the electron–phonon interactions. That is, the conventional BCS theory elucidating the mechanism of the occurrence of the macroscopic sized superconductivity has been established on the basis of the phenomenological London theory, which tries to explain the nondissipative diamagnetic currents in the microscopic sizes. On the other hand, the mechanism of the forming of the stable electronic structures with $\boldsymbol{p}_{\text{canonical}}=0$ assumed in the phenomenological London theory in the microscopic sized atoms and molecules has not been elucidated (Scheme 1). Even though the conventional BCS theory for the macroscopic sized superconducting materials has been established on the basis of the London theory for the nondissipative diamagnetic currents in the microscopic sized atoms and molecules, the nondissipative diamagnetic currents in the microscopic sized atoms and molecules

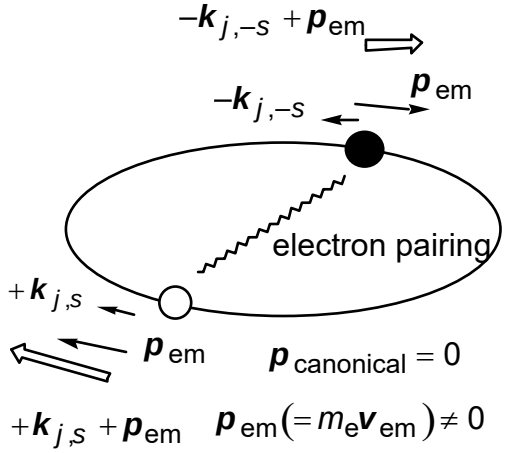

Scheme 1. Supercurrent in the microscopic sized one benzene molecule.

have not been considered as superconductivity (Scheme 1). In the previous research, we suggested that the Cooper pairs can be formed by the large valence–conduction band gaps ($\Delta E_{\text{HOMO–LUMO},N}$) as a consequence of the quantization of the orbitals by nature, and by the attractive Coulomb interactions between two electrons with opposite momentum and spins occupying the same orbitals via the positively charged nuclei [1–7]. We try to elucidate that the nondissipative diamagnetic currents in the microscopic sized atoms and molecules can be considered as superconductivity (Scheme 1), by considering the reason why the Meissner effect can be observed in superconductivity, in more detail, in this article.

3. Energy Level for the One and Two Electrons Systems

3.1 Zero Momentum Condensated States in the One- and Two-Electrons Systems

In the closed-shell electronic structure in superconductivity, two electrons occupying the same orbital j have the opposite momentum and spins ($\left|+\boldsymbol{k}_j\uparrow,-\boldsymbol{k}_j\downarrow\right\rangle$ and $\left|+\boldsymbol{k}_j\downarrow,-\boldsymbol{k}_j\uparrow\right\rangle$) by each other, and are condensated into the zero-momentum state (Bose–Einstein condensation), and therefore, there is the bosonic standing wave ($\left|\boldsymbol{k}_{\text{ground,two}}\right\rangle$) with zero momentum ($\boldsymbol{p}_{\text{canonical}}=0$) formed by two components of the fermionic traveling waves of two electrons (Fig. 1 (a)),

$$\left|\boldsymbol{k}_{\text{ground,two}}\right\rangle=c_{j\uparrow\downarrow}\left|+\boldsymbol{k}_j\uparrow,-\boldsymbol{k}_j\downarrow\right\rangle$$

International Journal of Scientific Engineering and Applied Science (IJSEAS) – Volume-3, Issue-4, April 2017
ISSN: 2395-3470
www.ijseas.com

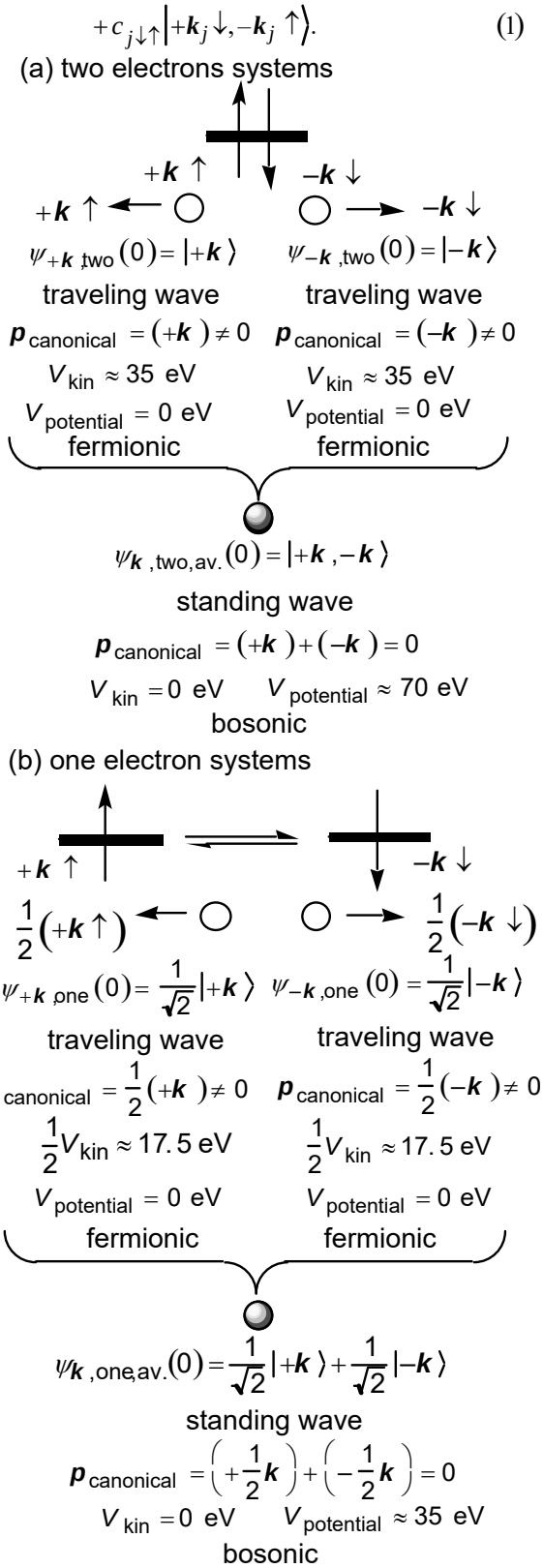

Fig. 1. Standing and traveling waves. (a) Two electrons systems. (b) One electron systems.

Since each fermionic electron ($\left|+\boldsymbol{k}_j\uparrow\right\rangle$ and $\left|-\boldsymbol{k}_j\downarrow\right\rangle$, and $\left|+\boldsymbol{k}_j\downarrow\right\rangle$ and $\left|-\boldsymbol{k}_j\uparrow\right\rangle$) has the kinetic energy of about 35 eV, the condensation energy for two electrons ($\left|\boldsymbol{k}_{\text{ground,two}}\right\rangle$) ($\boldsymbol{p}_{\text{canonical}}=0$) is very large, and usually is about 70 eV. This standing wave state ($\left|\boldsymbol{k}_{\text{ground,two}}\right\rangle$), related to the Cooper pair in superconductivity, is very rigid and stable because of the closed-shell electronic structure in the two-electrons systems ($\left|+\boldsymbol{k}_j\uparrow,-\boldsymbol{k}_j\downarrow\right\rangle$ and $\left|+\boldsymbol{k}_j\downarrow,-\boldsymbol{k}_j\uparrow\right\rangle$) (Fig. 1 (a)). This is closely related to the condensation of electrons into zero momentum state ($\boldsymbol{p}_{\text{canonical}}=0$) in one-electron system in the London theory in superconductivity, even though London could not elucidate how each electron can be condensated into the zero momentum state ($\boldsymbol{p}_{\text{canonical}}=0$).

Let us next consider how each electron can be condensated into the zero momentum state ($\boldsymbol{p}_{\text{canonical}}=0$) in one-electron systems. We can consider that this theory is applicable even for the one-electron system in the normal metals since there is no spontaneous electrical current and the magnetic moment in any direction without any applied electric and magnetic fields even in the normal metals. It should be noted that an electron is wave as well as particle. Therefore, in a similar way, even one electron partially occupying the same orbital j is formed by two components of the fermionic traveling waves with opposite momentum and spins ($\left|+\boldsymbol{k}_j\uparrow\right\rangle$ and $\left|-\boldsymbol{k}_j\downarrow\right\rangle$, $\left|+\boldsymbol{k}_j\downarrow\right\rangle$ and $\left|-\boldsymbol{k}_j\uparrow\right\rangle$) by each other, and is condensated into the bosonic zero-momentum state, and therefore, there is standing wave ground state ($\left|\boldsymbol{k}_{\text{ground,one}}\right\rangle$) with zero momentum ($\boldsymbol{p}_{\text{canonical}}=0$) and zero average kinetic energy under each applied external magnetic field (Fig. 1 (b)),

$$\left|\boldsymbol{k}_{\text{ground,one}}\right\rangle=c_{j\uparrow\downarrow}\left(\left|+\boldsymbol{k}_j\uparrow\right\rangle+\left|-\boldsymbol{k}_j\downarrow\right\rangle\right)+c_{j\downarrow\uparrow}\left(\left|+\boldsymbol{k}_j\downarrow\right\rangle+\left|-\boldsymbol{k}_j\uparrow\right\rangle\right) \quad (2)$$

Such condensation energy from the kinetic energy (V_{kin}) to the potential energy ($V_{\text{potential}}$) is very large, and usually is about 35 eV. Such condensation originates from the fact that two fermionic traveling waves with opposite direction, the kinetic energy of which is about 35 eV, form the bosonic standing wave, the kinetic energy of which is 0 eV. On the other hand, this standing wave ground state ($\left|\boldsymbol{k}_{\text{ground,one}}\right\rangle$) formed by only one electron ($\left|+\boldsymbol{k}_j\uparrow\right\rangle+\left|-\boldsymbol{k}_j\downarrow\right\rangle$ and $\left|+\boldsymbol{k}_j\downarrow\right\rangle+\left|-\boldsymbol{k}_j\uparrow\right\rangle$) is very fragile

and unstable even under the applied very small extra external magnetic field because of the opened-shell electronic structure in the one-electron system (Fig. 1 (b)).

3.2 Energy for the One Electron Systems

Without any applied magnetic or electric field (ground state), the energy ($E_{\mathrm{Fermi},\boldsymbol{k}_{\mathrm{HOCO}}\sigma}(0)$) for the fermionic states ($\psi_{\mathrm{Fermi},\boldsymbol{k}_{\mathrm{HOCO}}\sigma}(0)$) of an electron with spin σ occupying the highest occupied crystal orbital (HOCO) at 0 K can be expressed as follows (Fig. 1 (b)), according to the conventional solid state physics,

$$E_{\mathrm{Fermi},\boldsymbol{k}_{\mathrm{HOCO}}\sigma}(0) = V_{\mathrm{Coulomb},\mathrm{Fermi},\boldsymbol{k}_{\mathrm{HOCO}}\sigma}(0) + V_{\mathrm{kin},\mathrm{Fermi},\boldsymbol{k}_{\mathrm{HOCO}}\sigma}(0), \quad (3)$$

where the $V_{\mathrm{Coulomb},\mathrm{Fermi},\boldsymbol{k}_{\mathrm{HOCO}}\sigma}(0)$ value denotes the Coulomb energy between a fermionic electron with spin σ occupying the HOCO and all another nuclei and electrons, and the $V_{\mathrm{kin},\mathrm{Fermi},\boldsymbol{k}_{\mathrm{HOCO}}\sigma}(0)$ value denotes the kinetic energy for a fermionic electron with spin σ occupying the HOCO.

A boson has zero total momentum ($\boldsymbol{p}_{\mathrm{canonical}}(0)=0$) and kinetic energies ($V_{\mathrm{kin},\mathrm{Bose},\boldsymbol{k}_{\mathrm{HOCO}}\sigma}(0)=0$). Therefore, without any applied magnetic field (ground states; $\boldsymbol{p}_{\mathrm{canonical}}(0)=0$), the energy ($E_{\mathrm{Bose},\boldsymbol{k}_{\mathrm{HOCO}}\sigma}(0)$) for the bosonic electronic states ($\psi_{\mathrm{Bose},\boldsymbol{k}_{\mathrm{HOCO}}\sigma}(0)$) of an electron with spin σ occupying the HOCO can be expressed as (Fig. 1 (b)),

$$E_{\mathrm{Bose},\boldsymbol{k}_{\mathrm{HOCO}}\sigma}(0) = V_{\mathrm{Coulomb},\mathrm{Bose},\boldsymbol{k}_{\mathrm{HOCO}}\sigma} = V_{\mathrm{Coulomb},\mathrm{Fermi},\boldsymbol{k}_{\mathrm{HOCO}}\sigma}, \quad (4)$$

where the $V_{\mathrm{Coulomb},\mathrm{Bose},\boldsymbol{k}_{\mathrm{HOCO}}\sigma}(0)$ value denotes the Coulomb energy between a bosonic electron with spin σ occupying the HOCO and all another nuclei and electrons, and the $V_{\mathrm{kin},\mathrm{Bose},\boldsymbol{k}_{\mathrm{HOCO}}\sigma}(0)(=0)$ value denotes the kinetic energy for a bosonic electron with spin σ occupying the HOCO. As a consequence of the Bose–Einstein condensation, the kinetic energy ($V_{\mathrm{kin},\mathrm{Fermi},\boldsymbol{k}_{\mathrm{HOCO}}\sigma}(0)$) for a fermionic particle with $\boldsymbol{p}_{\mathrm{canonical}}(0)\neq 0$ has been converted to the potential energy ($V_{\mathrm{potential},\mathrm{Bose},\boldsymbol{k}_{\mathrm{HOCO}}\sigma}(0)$) for a bosonic particle with $\boldsymbol{p}_{\mathrm{canonical}}(0)=0$ (Fig. 1 (b)).

According to Refs. [1–7], we can consider that an electron formed by the two electronic states with opposite momentum and spins can be considered to have bosonic properties at the ground state, and the Bose–Einstein condensation energy ($\Delta E_{\mathrm{BE},\boldsymbol{k}_{\mathrm{HOCO}}\sigma}(0)$) from a fermionic electron ($\psi_{\mathrm{Fermi},\boldsymbol{k}_{\mathrm{HOCO}}\sigma}(0)$) to a bosonic electron ($\psi_{\mathrm{Bose},\boldsymbol{k}_{\mathrm{HOCO}}\sigma}(0)$) with spin σ occupying the HOCO can be expressed as (Fig. 1 (b)),

$$\Delta E_{\mathrm{BE},\boldsymbol{k}_{\mathrm{HOCO}}\sigma}(0) = E_{\mathrm{Fermi},\boldsymbol{k}_{\mathrm{HOCO}}\sigma}(0) - E_{\mathrm{Bose},\boldsymbol{k}_{\mathrm{HOCO}}\sigma}(0) = V_{\mathrm{kin},\mathrm{Fermi},\boldsymbol{k}_{\mathrm{HOCO}}\sigma}(0). \quad (5)$$

The $V_{\mathrm{kin},\mathrm{Fermi},\boldsymbol{k}_{\mathrm{HOCO}}\sigma}(0)$ values are usually very large (≈ 35 eV). That is, we have considered that an electron occupying an orbital in the ground state without any external fields, can become bosonic state ($|\boldsymbol{k}_{\mathrm{ground,HOCO,one}}\rangle$) with zero total momentum ($\boldsymbol{p}_{\mathrm{canonical}}(0)=0$) and kinetic energies ($V_{\mathrm{kin},\mathrm{Bose},\boldsymbol{k}_{\mathrm{HOCO}}\sigma}(0)=0$) formed by two components of the fermionic traveling waves ($|+\boldsymbol{k}_{\mathrm{HOCO}}\uparrow\rangle+|-\boldsymbol{k}_{\mathrm{HOCO}}\downarrow\rangle$ and $|+\boldsymbol{k}_{\mathrm{HOCO}}\downarrow\rangle+|-\boldsymbol{k}_{\mathrm{HOCO}}\uparrow\rangle$) with opposite momentum and spins [1–7]. Such stabilization energy of the bosonic standing wave states with respect to the two fermionic traveling wave states (i.e., Bose–Einstein condensation energy) originates from the disappearance of the kinetic energy ($\boldsymbol{p}_{\mathrm{canonical}}(0)=0$ and $V_{\mathrm{kin},\mathrm{Bose},\boldsymbol{k}_{\mathrm{HOCO}}\sigma}(0)=0$), and can be estimated to be $V_{\mathrm{kin},\mathrm{Fermi},\boldsymbol{k}_{\mathrm{HOCO}}\sigma}(0)$ (≈ 35 eV) (Fig. 1 (b)) [1–7].

3.3 Energy for the Two Electrons Systems

Without any applied magnetic field or electric field (ground state; $\boldsymbol{p}_{\mathrm{canonical}}(0)=0$), the energy ($E_{\mathrm{Fermi},\boldsymbol{k}_{\mathrm{HOCO}}\sigma\boldsymbol{k}'_{\mathrm{HOCO}}\sigma'}(0)$) for the fermionic states ($V_{\mathrm{kin},\mathrm{Fermi},\boldsymbol{k}_{\mathrm{HOCO}}\sigma\boldsymbol{k}'_{\mathrm{HOCO}}\sigma'}(0)\neq 0$) of two electrons occupying the HOCO ($\psi_{\mathrm{Fermi},\boldsymbol{k}_{\mathrm{HOCO}}\sigma\boldsymbol{k}'_{\mathrm{HOCO}}\sigma'}(0)$) can be expressed as follows (Fig. 1 (a)), according to the conventional solid state physics,

$$E_{\mathrm{Fermi},\boldsymbol{k}_{\mathrm{HOCO}}\sigma\boldsymbol{k}'_{\mathrm{HOCO}}\sigma'}(0) = 2V_{\mathrm{Coulomb},\mathrm{Fermi},\boldsymbol{k}_{\mathrm{HOCO}}\sigma}(0) + 2V_{\mathrm{kin},\mathrm{Fermi},\boldsymbol{k}_{\mathrm{HOCO}}\sigma}(0). \quad (6)$$

Furthermore, without any applied magnetic or electric field (ground states; $\boldsymbol{p}_{\mathrm{canonical}}(0)=0$), the energy ($E_{\mathrm{Bose},\pm\boldsymbol{k}_{\mathrm{HOCO}}\sigma\mp\boldsymbol{k}_{\mathrm{HOCO}}\sigma'}(0)$) for the bosonic electronic states ($V_{\mathrm{kin},\mathrm{Bose},\pm\boldsymbol{k}_{\mathrm{HOCO}}\sigma\mp\boldsymbol{k}_{\mathrm{HOCO}}\sigma'}(0)=0$) of two electrons ($\psi_{\mathrm{Bose},\pm\boldsymbol{k}_{\mathrm{HOCO}}\sigma\mp\boldsymbol{k}_{\mathrm{HOCO}}\sigma'}(0)$) can be expressed as (Fig. 1 (a)),

$$E_{\text{Bose},\pm \boldsymbol{k}_{\text{HOCO}}\sigma\mp\boldsymbol{k}_{\text{HOCO}}\sigma'}(0) = 2V_{\text{Coulomb,Fermi},\boldsymbol{k}_{\text{HOCO}}\sigma}(0). \quad (7)$$

Therefore, we can consider that a Cooper pair formed by two electrons with opposite momentum and spins can be considered to have bosonic properties at the ground state ($\boldsymbol{p}_{\text{canonical}}(0)=0$), and the Bose–Einstein condensation ($2\Delta E_{\text{BE}}(0)$) for two electrons from fermionic electrons ($\psi_{\text{Fermi},\boldsymbol{k}_{\text{HOCO}}\sigma\boldsymbol{k}'_{\text{HOCO}}\sigma'}(0)$) to a bosonic electron pair ($\psi_{\text{Bose},\pm\boldsymbol{k}_{\text{HOCO}}\sigma\mp\boldsymbol{k}_{\text{HOCO}}\sigma'}(0)$) can be expressed as (Fig. 1 (a)),

$$2\Delta E_{\text{BE}}(0) = E_{\text{Fermi},\boldsymbol{k}_{\text{HOCO}}\sigma\boldsymbol{k}'_{\text{HOCO}}\sigma'}(0) - E_{\text{Bose},\pm\boldsymbol{k}_{\text{HOCO}}\sigma\mp\boldsymbol{k}_{\text{HOCO}}\sigma'}(0) = 2V_{\text{kin,Fermi},\boldsymbol{k}_{\text{HOCO}}\sigma}(0) \approx 70 \text{ eV}. \quad (8)$$

That is, we can consider that two electrons occupying an orbital in the ground state without any external fields, can become bosonic state ($\left|\boldsymbol{k}_{\text{ground,HOCO,two}}\right\rangle$) with zero total momentum ($\boldsymbol{p}_{\text{canonical}}(0)=0$) and kinetic energies ($V_{\text{kin,Bose},\boldsymbol{k}_{\text{HOCO}}\sigma}(0)=0$) as a consequence of electron pairing between two fermionic electrons ($\left|+\boldsymbol{k}_{\text{HOCO}}\uparrow,-\boldsymbol{k}_{\text{HOCO}}\downarrow\right\rangle$ and $\left|+\boldsymbol{k}_{\text{HOCO}}\downarrow,-\boldsymbol{k}_{\text{HOCO}}\uparrow\right\rangle$) with opposite momentum and spins [1–7]. Such stabilization energy of the bosonic standing wave in two electrons with respect to the two fermionic traveling waves in two electrons (i.e., Bose–Einstein condensation energy) originates from the disappearance of the kinetic energy ($\boldsymbol{p}_{\text{canonical}}(0)=0$ and $V_{\text{kin,Bose},\boldsymbol{k}_{\text{HOCO}}\sigma}(0)=0$), and can be estimated to be $2V_{\text{kin,Fermi},\boldsymbol{k}_{\text{HOCO}}\sigma}(0)(\approx 70 \text{ eV})$ (Fig. 1 (a)) [1–7].

4. Energy Gap Forming in the Superconductivity

Let us next look into the energy gap formed by electron–phonon interactions in superconductivity.

4.1 One New Theory

The energy for the two fermionic electrons ($\psi_{\text{Fermi},\boldsymbol{k}_{\text{HOCO}}\sigma\boldsymbol{k}'_{\text{HOCO}}\sigma',\text{before}}(0)$) before electron–phonon interactions can be expressed as (Fig. 2),

$$E_{\text{Fermi},\boldsymbol{k}_{\text{HOCO}}\sigma\boldsymbol{k}'_{\text{HOCO}}\sigma',\text{before}}(0) = 2V_{\text{Coulomb,Fermi},\boldsymbol{k}_{\text{HOCO}}\sigma}(0) + 2V_{\text{kin,Fermi},\boldsymbol{k}_{\text{HOCO}}\sigma}(0), \quad (9)$$

and that for bosonic state ($\psi_{\text{Bose},\boldsymbol{k}_{\text{HOCO}}\sigma,\text{before}}(0)$ and $\psi_{\text{Bose},\boldsymbol{k}'_{\text{HOCO}}\sigma',\text{before}}(0)$) formed by the two bosonic

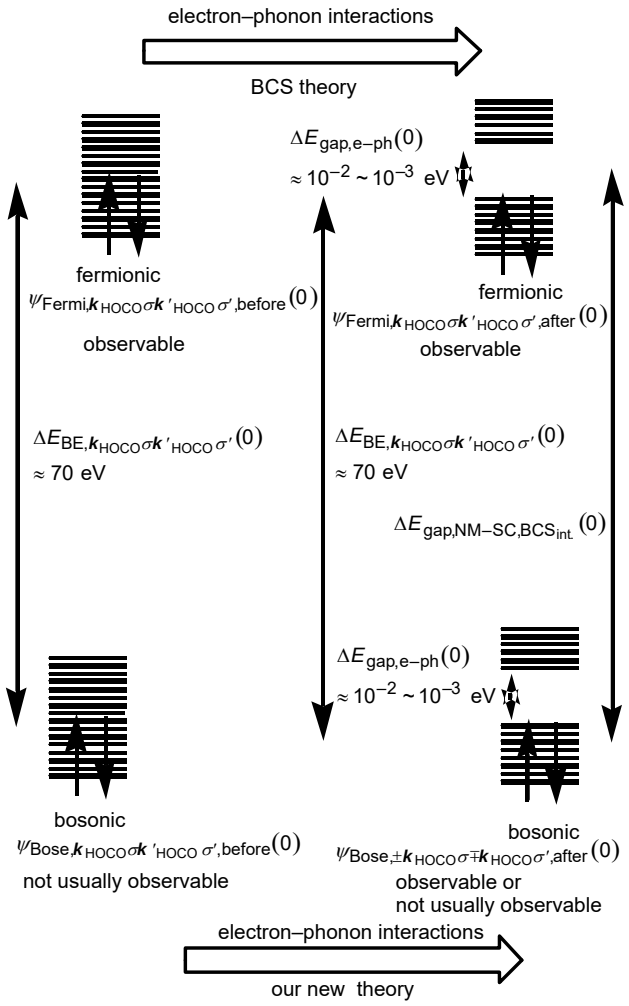

Fig. 2. The energy levels for the fermionic and bosonic electrons in the BCS theory and our theory.

electrons before electron–phonon interactions can be expressed as (Fig. 2),

$$2E_{\text{Bose},\boldsymbol{k}_{\text{HOCO}}\sigma,\text{before}}(0) = 2V_{\text{Coulomb,Fermi}}(0). \quad (10)$$

On the other hand, the energy for the two fermionic electrons ($\psi_{\text{Fermi},\boldsymbol{k}_{\text{HOCO}}\sigma\boldsymbol{k}'_{\text{HOCO}}\sigma',\text{after}}(0)$) after electron–phonon interactions can be expressed as (Fig. 2),

$$E_{\text{Fermi},\boldsymbol{k}_{\text{HOCO}}\sigma\boldsymbol{k}'_{\text{HOCO}}\sigma',\text{after}}(0) = 2V_{\text{Coulomb,Fermi},\boldsymbol{k}_{\text{HOCO}}\sigma}(0) + 2V_{\text{kin,Fermi},\boldsymbol{k}_{\text{HOCO}}\sigma}(0) - \Delta E_{\text{gap,e–ph}}(0), \quad (11)$$

and that for bosonic state ($\psi_{\text{Bose},\pm\boldsymbol{k}_{\text{HOCO}}\sigma\mp\boldsymbol{k}_{\text{HOCO}}\sigma',\text{after}}(0)$) formed by the two fermionic electrons after electron–phonon interactions can be expressed as (Fig. 2),

$$E_{\mathrm{Bose},\pm \boldsymbol{k}_{\mathrm{HOCO}}\sigma\mp\boldsymbol{k}_{\mathrm{HOCO}}\sigma',\mathrm{after}}(0) = 2V_{\mathrm{Coulomb,Fermi},\boldsymbol{k}_{\mathrm{HOCO}}\sigma}(0) - \Delta E_{\mathrm{gap,e-ph}}(0). \quad (12)$$

4.2 Problems in the Conventional BCS Theory

According to the conventional BCS theory, we consider that two fermionic electrons ($\psi_{\mathrm{Fermi},\boldsymbol{k}_{\mathrm{HOCO}}\sigma\boldsymbol{k}'_{\mathrm{HOCO}}\sigma',\mathrm{before}}(0)$) are condensated into one bosonic Cooper pair ($\psi_{\mathrm{Bose},\pm\boldsymbol{k}_{\mathrm{HOCO}}\sigma\mp\boldsymbol{k}_{\mathrm{HOCO}}\sigma',\mathrm{after}}(0)$) as a consequence of electron–phonon interactions, and at the same time, the Bose–Einstein condensation occurs. Obeying this interpretation, the energy difference ($\Delta E_{\mathrm{gap,NM-SC,BCS_{int.}}}(0)$) between them can be expressed as (Fig. 2),

$$\begin{aligned}&\Delta E_{\mathrm{gap,NM-SC,BCS_{int.}}}(0)\\ &= E_{\mathrm{Fermi},\boldsymbol{k}_{\mathrm{HOCO}}\sigma\boldsymbol{k}'_{\mathrm{HOCO}}\sigma',\mathrm{before}}(0)\\ &-E_{\mathrm{Bose},\pm\boldsymbol{k}_{\mathrm{HOCO}}\sigma\mp\boldsymbol{k}_{\mathrm{HOCO}}\sigma',\mathrm{after}}(0)\\ &= \Delta E_{\mathrm{gap,e-ph}}(0) + 2V_{\mathrm{kin,Fermi},\boldsymbol{k}_{\mathrm{HOCO}}\sigma}(0)\\ &= \Delta E_{\mathrm{gap,e-ph}}(0) + \Delta E_{\mathrm{BE},\boldsymbol{k}_{\mathrm{HOCO}}\sigma\boldsymbol{k}'_{\mathrm{HOCO}}\sigma'}(0). \quad (13)\end{aligned}$$

On the other hand, this interpretation contradicts the equation of the BCS theory itself. The usual $\Delta E_{\mathrm{gap,NM-SC,BCS_{calc.}}}(0)$ values estimated on the basis of the conventional BCS theory can be expressed as (Fig. 2),

$$\begin{aligned}&\Delta E_{\mathrm{gap,NM-SC,BCS_{calc.}}}(0)\\ &= E_{\mathrm{Fermi},\boldsymbol{k}_{\mathrm{HOCO}}\sigma\boldsymbol{k}'_{\mathrm{HOCO}}\sigma',\mathrm{before}}(0)\\ &-E_{\mathrm{Fermi},\boldsymbol{k}_{\mathrm{HOCO}}\sigma\boldsymbol{k}'_{\mathrm{HOCO}}\sigma',\mathrm{after}}(0)\\ &= \Delta E_{\mathrm{gap,e-ph}}(0). \quad (14)\end{aligned}$$

In such a case, the $\Delta E_{\mathrm{gap,NM-SC,BCS_{int.}}}(0)$ values are very large, and are not estimated to be the same with the $\Delta E_{\mathrm{gap,NM-SC,BCS_{calc.}}}(0)$ values estimated on the basis of the conventional BCS theory. In the BCS theory, unstable two electrons before the electron–phonon interactions in the normal metallic states are considered to be fermionic while the stable two electrons after electron–phonon interactions are considered to be bosonic (Fig. 2). That is, estimation ($\Delta E_{\mathrm{gap,NM-SC,BCS_{calc.}}}(0)$) and interpretation ($\Delta E_{\mathrm{gap,NM-SC,BCS_{int.}}}(0)$) of the physical parameters for $\Delta E_{\mathrm{gap,NM-SC}}(0)$ are somewhat ambiguous in the conventional BCS theory. Furthermore, the $\Delta E_{\mathrm{gap,NM-SC,BCS_{calc.}}}(0)$ and $\Delta E_{\mathrm{gap,e-ph}}(0)$ values have been called the "Bose–Einstein condensation energy ($\Delta E_{\mathrm{BE},\boldsymbol{k}_{\mathrm{HOCO}}\sigma\boldsymbol{k}'_{\mathrm{HOCO}}\sigma'}(0)$)" in the conventional BCS theory. It is also ambiguous definition because the $\Delta E_{\mathrm{gap,NM-SC,BCS_{calc.}}}(0)$ and $\Delta E_{\mathrm{gap,e-ph}}(0)$ values are not related to the conversion from the fermionic states to the bosonic states ($\Delta E_{\mathrm{BE},\boldsymbol{k}_{\mathrm{HOCO}}\sigma\boldsymbol{k}'_{\mathrm{HOCO}}\sigma'}(0)$), but are related to the energy difference ($\Delta E_{\mathrm{gap,e-ph}}(0)$) between the stable fermionic two electrons after electron–phonon interactions ($\psi_{\mathrm{Fermi},\boldsymbol{k}_{\mathrm{HOCO}}\sigma\boldsymbol{k}'_{\mathrm{HOCO}}\sigma',\mathrm{after}}(0)$) and the unstable fermionic two electrons before electron–phonon interactions ($\psi_{\mathrm{Fermi},\boldsymbol{k}_{\mathrm{HOCO}}\sigma\boldsymbol{k}'_{\mathrm{HOCO}}\sigma',\mathrm{before}}(0)$), which are actually observed (Fig. 2). The $\Delta E_{\mathrm{BE},\boldsymbol{k}_{\mathrm{HOCO}}\sigma\boldsymbol{k}'_{\mathrm{HOCO}}\sigma'}(0)$ values are usually very large (≈ 70 eV), on the other hand, the $\Delta E_{\mathrm{gap,NM-SC,obs.}}(0)$ and $\Delta E_{\mathrm{gap,e-ph}}(0)$ values are usually observed to be very small ($\approx 10^{-2} \sim 10^{-3}$ eV). Therefore, we should reconsider the interpretation of the BCS theory, as shown below.

4.3 New Interpretation of the Bose–Einstein Condensation in Superconductivity

In the BCS theory, unstable two electrons before the electron–phonon interactions in the normal metallic states are considered to be fermionic while the stable two electrons after electron–phonon interactions are considered to be bosonic (Fig. 2). If we consider that the stable two electrons after electron–phonon interactions as well as the unstable two electrons before the electron–phonon interactions are fermionic, the $\Delta E_{\mathrm{gap,NM-SC,BCS_{calc.}}}(0)$ values are estimated to be the same with the $\Delta E_{\mathrm{gap,e-ph}}(0)$ values, as in Eq. (14) (Fig. 2). This is the equation (Eq. (14)) appearing in the conventional BCS theory and actually observed physical parameters,

$$\begin{aligned}\Delta E_{\mathrm{gap,NM-SC,obs.}}(0) &= \Delta E_{\mathrm{gap,NM-SC,BCS_{calc.}}}(0)\\ &= \Delta E_{\mathrm{gap,e-ph}}(0). \quad (15)\end{aligned}$$

That is, we should consider that the Bose–Einstein condensation occurs after electron–phonon interactions ($\Delta E_{\mathrm{gap,e-ph}}(0)$) are completed, and the Bose–Einstein condensation energy, can be expressed as $\Delta E_{\mathrm{BE},\boldsymbol{k}_{\mathrm{HOCO}}\sigma\boldsymbol{k}'_{\mathrm{HOCO}}\sigma'}(0)\left(= 2V_{\mathrm{kin,Fermi},\boldsymbol{k}_{\mathrm{HOCO}}\sigma}(0) \approx 70\ \mathrm{eV}\right)$ (Fig. 2),

$$\begin{aligned}&\Delta E_{\mathrm{BE},\boldsymbol{k}_{\mathrm{HOCO}}\sigma\boldsymbol{k}'_{\mathrm{HOCO}}\sigma'}(0)\\ &= E_{\mathrm{Fermi},\boldsymbol{k}_{\mathrm{HOCO}}\sigma\boldsymbol{k}'_{\mathrm{HOCO}}\sigma',\mathrm{before}}(0)\\ &-2E_{\mathrm{Bose},\boldsymbol{k}_{\mathrm{HOCO}}\sigma,\mathrm{before}}(0)\\ &= 2V_{\mathrm{kin,Fermi},\boldsymbol{k}_{\mathrm{HOCO}}\sigma}(0) \approx 70\ \mathrm{eV}. \quad (16)\end{aligned}$$

The $\Delta E_{\mathrm{gap,NM-SC}}(0)$ and $\Delta E_{\mathrm{gap,e-ph}}(0)$ values appearing in the BCS theory do not denote the Bose–Einstein condensation energy but denote the stabilization energy of the two fermionic electrons in the closed-shell electronic structure after electron–phonon interactions ($E_{\mathrm{Fermi},\boldsymbol{k}_{\mathrm{HOCO}}\sigma\boldsymbol{k}'_{\mathrm{HOCO}}\sigma',\mathrm{after}}(0)$) with respect to the two fermionic electrons in the opened-shell electronic structure ($E_{\mathrm{Fermi},\boldsymbol{k}_{\mathrm{HOCO}}\sigma\boldsymbol{k}'_{\mathrm{HOCO}}\sigma',\mathrm{before}}(0)$) (Fig. 2). We should consider that after electron–phonon interactions are completed ($E_{\mathrm{Fermi},\boldsymbol{k}_{\mathrm{HOCO}}\sigma\boldsymbol{k}'_{\mathrm{HOCO}}\sigma',\mathrm{after}}(0)$), the Bose–Einstein condensation can occur ($E_{\mathrm{Bose},\pm\boldsymbol{k}_{\mathrm{HOCO}}\sigma\mp\boldsymbol{k}_{\mathrm{HOCO}}\sigma',\mathrm{after}}(0)$), in the BCS theory. In such a case, the Bose–Einstein condensation energy ($\Delta E_{\mathrm{BE},\boldsymbol{k}_{\mathrm{HOCO}}\sigma\boldsymbol{k}'_{\mathrm{HOCO}}\sigma'}(0)$) denotes the stabilization energy of a bosonic Cooper pair in the closed-shell electronic structure after electron–phonon interactions ($E_{\mathrm{Bose},\pm\boldsymbol{k}_{\mathrm{HOCO}}\sigma\mp\boldsymbol{k}_{\mathrm{HOCO}}\sigma',\mathrm{after}}(0)$) with respect to the two fermionic electrons in the closed-shell electronic structure after electron–phonon interactions ($E_{\mathrm{Fermi},\boldsymbol{k}_{\mathrm{HOCO}}\sigma\boldsymbol{k}'_{\mathrm{HOCO}}\sigma',\mathrm{after}}(0)$) (Fig. 2).

On the other hand, according to our theory, the already condensated two bosonic electrons ($2E_{\mathrm{Bose},\boldsymbol{k}_{\mathrm{HOCO}}\sigma,\mathrm{before}}(0)$) are converted to the already condensated one bosonic Cooper pair ($E_{\mathrm{Bose},\pm\boldsymbol{k}_{\mathrm{HOCO}}\sigma\mp\boldsymbol{k}_{\mathrm{HOCO}}\sigma',\mathrm{after}}(0)$) as a consequence of the electron–phonon interactions ($\Delta E_{\mathrm{gap,e-ph}}(0)$) (Fig. 2),

$$\begin{aligned}&\Delta E_{\mathrm{gap,NM-SC,our\ theory}}(0)\\&=2E_{\mathrm{Bose},\boldsymbol{k}_{\mathrm{HOCO}}\sigma,\mathrm{before}}(0)\\&-E_{\mathrm{Bose},\pm\boldsymbol{k}_{\mathrm{HOCO}}\sigma\mp\boldsymbol{k}_{\mathrm{HOCO}}\sigma',\mathrm{after}}(0)\\&=\Delta E_{\mathrm{gap,e-ph}}(0).\end{aligned}\qquad(17)$$

$$\begin{aligned}&\Delta E_{\mathrm{BE},\boldsymbol{k}_{\mathrm{HOCO}}\sigma\boldsymbol{k}'_{\mathrm{HOCO}}\sigma'}(0)\\&=E_{\mathrm{Fermi},\boldsymbol{k}_{\mathrm{HOCO}}\sigma\boldsymbol{k}'_{\mathrm{HOCO}}\sigma',\mathrm{after}}(0)\\&-E_{\mathrm{Bose},\pm\boldsymbol{k}_{\mathrm{HOCO}}\sigma\mp\boldsymbol{k}_{\mathrm{HOCO}}\sigma',\mathrm{after}}(0)\\&\approx E_{\mathrm{Fermi},\boldsymbol{k}_{\mathrm{HOCO}}\sigma\boldsymbol{k}'_{\mathrm{HOCO}}\sigma',\mathrm{before}}(0)\\&-2E_{\mathrm{Bose},\boldsymbol{k}_{\mathrm{HOCO}}\sigma,\mathrm{before}}(0)\\&=2V_{\mathrm{kin,Fermi},\boldsymbol{k}_{\mathrm{HOCO}}\sigma}(0)\approx 70\ \mathrm{eV}.\end{aligned}\qquad(18)$$

Our theory ($\Delta E_{\mathrm{gap,NM-SC,our\ theory}}(0)$) can well explain the equation ($\Delta E_{\mathrm{gap,NM-SC,BCS_{calc.}}}(0)$) in the BCS theory. According to our theory, two electrons before electron–phonon interactions in the normal metallic states ($2E_{\mathrm{Bose},\boldsymbol{k}_{\mathrm{HOCO}}\sigma,\mathrm{before}}(0)$) are also bosonic, and we can estimate the $\Delta E_{\mathrm{gap,NM-SC}}(0)$ values as follows. We consider that the already condensated two bosonic electrons ($2E_{\mathrm{Bose},\boldsymbol{k}_{\mathrm{HOCO}}\sigma,\mathrm{before}}(0)$) are converted to the already condensated one bosonic Cooper pair ($E_{\mathrm{Bose},\pm\boldsymbol{k}_{\mathrm{HOCO}}\sigma\mp\boldsymbol{k}_{\mathrm{HOCO}}\sigma',\mathrm{after}}(0)$) as a consequence of the electron–phonon interactions ($\Delta E_{\mathrm{gap,e-ph}}(0)$) (Fig. 2). In this case, the $\Delta E_{\mathrm{gap,NM-SC}}(0)$ value becomes the same with the $\Delta E_{\mathrm{gap,e-ph}}(0)$ value. This is because two electrons in the normal metallic states as well as the superconducting states are considered to be bosonic, and the $\Delta E_{\mathrm{BE},\boldsymbol{k}_{\mathrm{HOCO}}\sigma\boldsymbol{k}'_{\mathrm{HOCO}}\sigma'}(0)$ values for the unstable two bosonic electrons before electron–phonon interactions ($2E_{\mathrm{Bose},\boldsymbol{k}_{\mathrm{HOCO}}\sigma,\mathrm{before}}(0)$) are the same with that for the stable bosonic Cooper pair after electron–phonon interactions ($E_{\mathrm{Bose},\pm\boldsymbol{k}_{\mathrm{HOCO}}\sigma\mp\boldsymbol{k}_{\mathrm{HOCO}}\sigma',\mathrm{after}}(0)$) (Fig. 2). However, as we described above, we cannot usually observe bosonic electron (Eq. (10)) but can usually observe fermionic electron (Eq. (9)), in particular, when the orbitals occupied by electrons are changed. Therefore, we usually observe the physical parameters estimated on the basis of the Fermi particles (Eq. (9)) in the conventional solid state physics (Fig. 2).

Let us next look into the observation of the electron–phonon interaction processes. The process from the destruction of the already condensated two bosonic electrons ($2E_{\mathrm{Bose},\boldsymbol{k}_{\mathrm{HOCO}}\sigma,\mathrm{before}}(0)$) (formation of the two fermionic electrons ($E_{\mathrm{Fermi},\boldsymbol{k}_{\mathrm{HOCO}}\sigma\boldsymbol{k}'_{\mathrm{HOCO}}\sigma',\mathrm{before}}(0)$)) in the opened-shell electronic structure to the formation of the two fermionic electrons ($E_{\mathrm{Fermi},\boldsymbol{k}_{\mathrm{HOCO}}\sigma\boldsymbol{k}'_{\mathrm{HOCO}}\sigma',\mathrm{after}}(0)$) in the closed-shell electronic structure as a consequence of the electron–phonon interactions is considered in the BCS theory, and is usually observed (Fig. 2). When we try to observe the electron–phonon processes, we cannot usually observe the bosonic metallic states before electron–phonon interactions ($2E_{\mathrm{Bose},\boldsymbol{k}_{\mathrm{HOCO}}\sigma,\mathrm{before}}(0)$) and the bosonic superconducting states after electron-phonon interactions ($E_{\mathrm{Bose},\pm\boldsymbol{k}_{\mathrm{HOCO}}\sigma\mp\boldsymbol{k}_{\mathrm{HOCO}}\sigma',\mathrm{after}}(0)$) (Fig. 2).

5. Relationships between the Fermionic and Bosonic Properties in Two Electrons Systems

Let us look into the two electrons with opposite momentum and spins occupying the same orbitals in the closed-shell electronic structures with large energy gaps between the occupied and unoccupied orbitals in various small sized materials such as the neutral He atom and benzene. There are two possible electronic properties, i.e., (i) two fermionic intrinsic insulating particles states (the most probable from the point of view of the conventional solid state physics) (Fig. 3 (a)), and (ii) one bosonic superconducting particle states (Cooper pair) (predicted from our theory) (Fig. 3 (b)). According to the

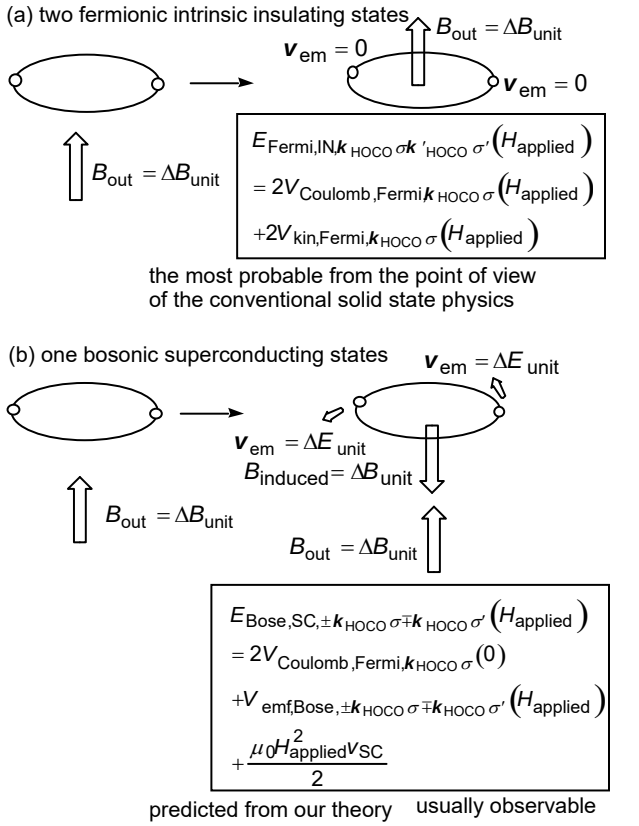

Fig. 3. Two electronic structures. (a) Two fermionic intrinsic insulating states. (b) One bosonic superconducting states. (c) Energy difference between the two fermionic insulating states and the one bosonic superconducting states.

conventional solid state physics, the two fermionic intrinsic insulating particles are predicted (Fig. 3 (a)), on the other hand, we usually observe the nondissipative diamagnetic current states (one bosonic superconducting particle states) (Fig. 3 (b)). This is the problem we must solve in this article.

5.1 Two Fermionic Intrinsic Insulating Particles States

Let us first look into the two fermionic intrinsic insulating particles states ($\psi_{two,Fermi,IN}$), which obey the Pauli exclusion principle (Figs. 1 (a) and 3 (a)),

$$\left|\boldsymbol{k}_{IN,two}\right\rangle = c_{HOCO\uparrow\downarrow}\left(\left|+\boldsymbol{k}_{HOCO}\uparrow\right\rangle + \left|-\boldsymbol{k}_{HOCO}\downarrow\right\rangle\right) + c_{HOCO\downarrow\uparrow}\left(\left|+\boldsymbol{k}_{HOCO}\downarrow\right\rangle + \left|-\boldsymbol{k}_{HOCO}\uparrow\right\rangle\right) \quad (19)$$

In the electronic states, there are independent two fermionic electrons with opposite momentum and spins occupying the same orbitals in the closed-shell electronic structures with large energy gaps between the occupied and unoccupied orbitals. Furthermore, these electronic states are not changed even under the applied magnetic field $H_{applied}$, and the magnetic fields are not expelled by these two electrons (Fig. 3 (a)). This electronic state can be predicted from the point of view of the conventional solid state physics since it is reasonable to consider that the total momentum of two fermionic electrons in the closed-shell electronic structure with large energy gaps between the occupied and unoccupied orbitals cannot be easily changed by the applied magnetic field $H_{applied}$ (Fig. 3 (a)). However, we usually observe the nondissipative diamagnetic current states (not intrinsic insulating states) (Fig. 3 (b)). The magnetic field as well as the electric field (or electromotive force) cannot be expelled from the insulating specimen.

5.2 One Bosonic Superconducting Particle States

Let us next look into the one bosonic superconducting particles states (Cooper pairs) ($\psi_{two,Bose,SC}$) (Fig. 3 (b)). In the electronic states, there is a bound particle formed by two electrons with opposite momentum and spins occupying the same orbitals in the closed-shell electronic structures with finite energy gaps between the occupied and unoccupied orbitals (Fig. 3 (b)),

$$\left|\boldsymbol{k}_{SC,two}\right\rangle = c_{HOCO\uparrow\downarrow}\left|+\boldsymbol{k}_{HOCO}\uparrow,-\boldsymbol{k}_{HOCO}\downarrow\right\rangle + c_{HOCO\downarrow\uparrow}\left|+\boldsymbol{k}_{HOCO}\downarrow,-\boldsymbol{k}_{HOCO}\uparrow\right\rangle. \quad (20)$$

These electronic states are changed under the applied magnetic field $H_{applied}$, and the magnetic field are expelled by these two electrons (Fig. 3 (b)). On the other hand, this electronic state cannot be predicted from the point of view of the conventional solid state physics since it is reasonable to consider that the total momentum states

of two electrons in the closed-shell electronic structure with large energy gaps between the occupied and unoccupied orbitals cannot be easily changed by the applied magnetic field H_{applied} (Fig. 3 (a)). However, we usually observe the nondissipative diamagnetic current states (not intrinsic insulating states) (Fig. 3 (b)). The magnetic field as well as the electric field (or electromotive force) can be expelled from the superconducting specimen.

6. The Mechanism of the Bose–Einstein Condensation in Two Electrons Systems

6.1 Two Fermionic Intrinsic Insulating Particles States

Let us next discuss why two electrons with opposite momentum and spins occupying the same orbital in the closed-shell electronic structures with large energy gaps between the occupied and unoccupied orbitals can be in the Bose–Einstein condensation (Figs. 1 (a) and 3 (b)). We first consider that two electrons with opposite momentum and spins occupying the same orbital in the closed-shell electronic structures with large energy gap between the occupied and unoccupied orbitals move independently as two Fermi particles ($\psi_{\text{two,Fermi,IN}}$) (Figs. 1 (a) and 3 (a)).

When very small magnetic field (H_{applied}) is applied, the energy ($E_{\text{Fermi,IN},\boldsymbol{k}_{\text{HOCO}}\sigma\boldsymbol{k}'_{\text{HOCO}}\sigma'}\left(H_{\text{applied}}\right)$) for the two fermionic electron systems can be expressed as

$$\begin{aligned}&E_{\text{Fermi,IN},\boldsymbol{k}_{\text{HOCO}}\sigma\boldsymbol{k}'_{\text{HOCO}}\sigma'}\left(H_{\text{applied}}\right)\\&=2V_{\text{Coulomb,Fermi},\boldsymbol{k}_{\text{HOCO}}\sigma}\left(H_{\text{applied}}\right)\\&+2V_{\text{kin,Fermi},\boldsymbol{k}_{\text{HOCO}}\sigma}\left(H_{\text{applied}}\right)\end{aligned}\qquad(21)$$

where the $E_{\text{Fermi,IN},\boldsymbol{k}_{\text{HOCO}}\sigma\boldsymbol{k}'_{\text{HOCO}}\sigma'}\left(H_{\text{applied}}\right)$ value denotes the energy level for two electrons, and the $V_{\text{Coulomb,Fermi},\boldsymbol{k}_{\text{HOCO}}\sigma}\left(H_{\text{applied}}\right)$ and $V_{\text{kin,Fermi},\boldsymbol{k}_{\text{HOCO}}\sigma}\left(H_{\text{applied}}\right)$ values denote the Coulomb energy and the kinetic energy for an electron occupying the HOCO, respectively. In the two fermionic systems, two electrons are not equivalent, and these two electrons independently behave as two Fermi particles, and thus we must consider the $V_{\text{kin,Fermi},\boldsymbol{k}_{\text{HOCO}}\sigma}\left(H_{\text{applied}}\right)(\neq 0)$ values as well as the $V_{\text{Coulomb,Fermi},\boldsymbol{k}_{\text{HOCO}}\sigma}\left(H_{\text{applied}}\right)$ values (Fig. 1 (a)).

6.2 Superconducting States as a Consequence of the Bose–Einstein Condensation

In a similar way, the energy ($E_{\text{Bose,SC},\pm\boldsymbol{k}_{\text{HOCO}}\sigma\mp\boldsymbol{k}_{\text{HOCO}}\sigma'}\left(H_{\text{applied}}\right)$) for the one bosonic electron systems under the applied magnetic field H_{applied} can be expressed as (Fig. 3 (b)),

$$\begin{aligned}&E_{\text{Bose,SC},\pm\boldsymbol{k}_{\text{HOCO}}\sigma\mp\boldsymbol{k}_{\text{HOCO}}\sigma'}\left(H_{\text{applied}}\right)\\&=V_{\text{Coulomb,Bose},\pm\boldsymbol{k}_{\text{HOCO}}\sigma\mp\boldsymbol{k}_{\text{HOCO}}\sigma'}\left(H_{\text{applied}}\right)\\&+V_{H_{\text{induced}}}\left(H_{\text{applied}}\right)\\&=2V_{\text{Coulomb,Fermi},\boldsymbol{k}_{\text{HOCO}}\sigma}(0)\\&+V_{\text{emf,Bose},\pm\boldsymbol{k}_{\text{HOCO}}\sigma\mp\boldsymbol{k}_{\text{HOCO}}\sigma'}\left(H_{\text{applied}}\right)\\&+V_{H_{\text{induced}}}\left(H_{\text{applied}}\right)\end{aligned}\qquad(22)$$

$$V_{H_{\text{induced}}}\left(H_{\text{applied}}\right)=\frac{\mu_0 H_{\text{applied}}^2 v_{\text{SC}}}{2},\qquad(23)$$

where the $V_{\text{Coulomb,Bose},\pm\boldsymbol{k}_{\text{HOCO}}\sigma\mp\boldsymbol{k}_{\text{HOCO}}\sigma'}\left(H_{\text{applied}}\right)$ and $V_{\text{kin,Bose},\pm\boldsymbol{k}_{\text{HOCO}}\sigma\mp\boldsymbol{k}_{\text{HOCO}}\sigma'}\left(H_{\text{applied}}\right)$ values denote the Coulomb and kinetic energies for two electrons occupying the HOCO, respectively, the v_{SC} denotes volume of the superconductor, and the μ_0 denotes the magnetic permeability in vacuum. Furthermore, the $V_{\text{emf,Bose},\pm\boldsymbol{k}_{\text{HOCO}}\sigma\mp\boldsymbol{k}_{\text{HOCO}}\sigma'}\left(H_{\text{applied}}\right)$ value denotes the kinetic energy of an electron pair as a consequence of the electromotive forces.

6.3 Energy Difference between the Two Fermionic Insulating States and the One Bosonic Superconducting States

Let us next compare the $E_{\text{Fermi,IN},\boldsymbol{k}_{\text{HOCO}}\sigma\boldsymbol{k}'_{\text{HOCO}}\sigma'}\left(H_{\text{applied}}\right)$ values with the $E_{\text{Bose,SC},\pm\boldsymbol{k}_{\text{HOCO}}\sigma\mp\boldsymbol{k}_{\text{HOCO}}\sigma'}\left(H_{\text{applied}}\right)$ values (Fig. 3). The energy difference ($\Delta E_{\text{SC-IN}}\left(H_{\text{applied}}\right)$) between the two fermionic insulating particle states ($E_{\text{Fermi,IN},\boldsymbol{k}_{\text{HOCO}}\sigma\boldsymbol{k}'_{\text{HOCO}}\sigma'}\left(H_{\text{applied}}\right)$) and the one bosonic superconducting states ($E_{\text{Bose,SC},\pm\boldsymbol{k}_{\text{HOCO}}\sigma\mp\boldsymbol{k}_{\text{HOCO}}\sigma'}\left(H_{\text{applied}}\right)$) under the applied magnetic field H_{applied} can be expressed as

$$\begin{aligned}&\Delta E_{\text{SC-IN}}\left(H_{\text{applied}}\right)\\&=E_{\text{Bose,SC},\pm\boldsymbol{k}_{\text{HOCO}}\sigma\mp\boldsymbol{k}_{\text{HOCO}}\sigma'}\left(H_{\text{applied}}\right)\\&-E_{\text{Fermi,IN},\boldsymbol{k}_{\text{HOCO}}\sigma\boldsymbol{k}'_{\text{HOCO}}\sigma'}\left(H_{\text{applied}}\right)\end{aligned}$$

$$= V_{H_{\text{induced}}}\left(H_{\text{applied}}\right) - 2V_{\text{kin, Fermi, }\boldsymbol{k}_{\text{HOCO}}\sigma}\left(H_{\text{applied}}\right) << 0. \quad (24)$$

The $2V_{\text{kin,Fermi,}\boldsymbol{k}_{\text{HOCO}}\sigma}\left(H_{\text{applied}}\right)$ values are usually very large (≈ 70 eV), and thus are much larger than the $V_{H_{\text{induced}}}\left(H_{\text{applied}}\right)$ values (usually in the order of $10^{-2} \sim 10^{-3}$ eV). Therefore, it is clear from the calculated results that the $E_{\text{Bose,SC,}\pm\boldsymbol{k}_{\text{HOCO}}\sigma\mp\boldsymbol{k}_{\text{HOCO}}\sigma'}\left(H_{\text{applied}}\right)$ values are much smaller than the $E_{\text{Fermi, IN,}\boldsymbol{k}_{\text{HOCO}}\sigma\boldsymbol{k}'_{\text{HOCO}}\sigma'}\left(H_{\text{applied}}\right)$ values, and thus the one bosonic superconducting particle states ($\psi_{\text{two,Bose, SC}}$) are much more stable than the two fermionic insulating states ($\psi_{\text{two,Fermi,IN}}$) (Fig. 3 (c)). It can be also understood from the fact that the superconducting states ($\psi_{\text{two,Bose, SC}}$) are stable and thus the stable one bosonic superconducting state ($\psi_{\text{two,Bose, SC}}$) are not converted into the unstable two fermionic intrinsic insulating states ($\psi_{\text{two,Fermi,IN}}$) via photon emission (Joule's heats) even under the constant applied magnetic field H_{applied} . Therefore, the nondissipative diamagnetic currents in the microscopic sized molecules as well as the macroscopic sized superconductivity can be explained by one bosonic superconducting states ($\psi_{\text{two,Bose, SC}}$) (Cooper pairs) (Fig. 3 (b)).

It should be noted that since there are equivalent two electrons with opposite momentum and spins, the total momentum of a Cooper pair can be also zero ($\boldsymbol{p}_{\text{canonical, HOCO}} = \left(+\boldsymbol{k}_{\text{HOCO}}\uparrow\right)+\left(-\boldsymbol{k}_{\text{HOCO}}\downarrow\right)= 0$), and thus the $V_{\text{kin, Cooper pair, }N}\left(+\boldsymbol{k}_{\text{HOMO}}\uparrow,-\boldsymbol{k}_{\text{HOMO}}\downarrow\right)$ value can be zero (Fig. 1). That is, the kinetic energy, which generally reduces the destruction energy of the bosonic Cooper pairs, and is compensated by the Coulomb energy ($V_{\text{Coulomb,}N}\left(\boldsymbol{k}_{\text{HOMO}}\sigma,\boldsymbol{k}_{\text{HOMO}}{}'\sigma'\right)$), does not play a role in the decision of the destruction energy of the bosonic Cooper pairs. This is because the kinetic energy for fermionic state is converted to the potential energy for bosonic state (Fig. 1 (a)). The Cooper pair can be formed by the Coulomb interactions between two electrons with opposite momentum and spins occupying the same orbitals via the positive charges of the nuclei. This is the reason why the $E_{\text{Bose,SC,}\pm\boldsymbol{k}_{\text{HOCO}}\sigma\mp\boldsymbol{k}_{\text{HOCO}}\sigma'}\left(H_{\text{applied}}\right)$ values are much smaller than the $E_{\text{Fermi, IN,}\boldsymbol{k}_{\text{HOCO}}\sigma\boldsymbol{k}'_{\text{HOCO}}\sigma'}\left(H_{\text{applied}}\right)$ values, and the reason why the bosonic particle ($\psi_{\text{Bose,SC,}\pm\boldsymbol{k}_{\text{HOCO}}\sigma\mp\boldsymbol{k}_{\text{HOCO}}\sigma'}\left(H_{\text{applied}}\right)$) is much more stable than two fermionic particles ($\psi_{\text{Fermi,IN,}\boldsymbol{k}_{\text{HOCO}}\sigma\boldsymbol{k}'_{\text{HOCO}}\sigma'}\left(H_{\text{applied}}\right)$) ($\Delta E_{\text{SC-IN}}\left(H_{\text{applied}}\right) << 0$) (Fig. 3 (c)). Furthermore, this is the reason why the Bose–Einstein condensation occurs in the closed-shell electronic structures with finite energy gaps between the occupied and unoccupied orbitals, and thus the reason why we usually observe the nondissipative diamagnetic currents in the microscopic sized atoms and molecules as well as in the macroscopic sized superconductivity (Fig. 3 (b)).

These calculated results can be also understood from the fact that we usually observe the supercurrent states ($\psi_{\text{Bose,SC,}\pm\boldsymbol{k}_{\text{HOCO}}\sigma\mp\boldsymbol{k}_{\text{HOCO}}\sigma'}\left(H_{\text{applied}}\right)$) (Fig. 3 (b)), rather than the intrinsic insulating states ($\psi_{\text{Fermi,IN,}\boldsymbol{k}_{\text{HOCO}}\sigma\boldsymbol{k}'_{\text{HOCO}}\sigma'}\left(H_{\text{applied}}\right)$) (Fig. 3 (a)). Furthermore, we can also say that the intrinsic insulators ($\psi_{\text{Fermi,IN,}\boldsymbol{k}_{\text{HOCO}}\sigma\boldsymbol{k}'_{\text{HOCO}}\sigma'}\left(H_{\text{applied}}\right)$) formed by two fermionic particle states in the closed-shell electronic structures with finite energy gaps between the occupied and unoccupied orbitals, which has been believed to exist from the point of view of solid state physics (Fig. 3 (a)), do not usually exist.

We can conclude that the kinetic energy $2V_{\text{kin,Fermi,}\boldsymbol{k}_{\text{HOCO}}\sigma}(0)$ for the $\psi_{\text{Fermi,IN,}\boldsymbol{k}_{\text{HOCO}}\sigma\boldsymbol{k}'_{\text{HOCO}}\sigma'}\left(H_{\text{applied}}\right)$ state is converted to the internal potential energy for the $\psi_{\text{Bose,SC,}\pm\boldsymbol{k}_{\text{HOCO}}\sigma\mp\boldsymbol{k}_{\text{HOCO}}\sigma'}\left(H_{\text{applied}}\right)$ state, as a consequence of the Bose–Einstein condensation (Fig. 1 (a)), by which the bosonic states ($\psi_{\text{Bose,SC,}\pm\boldsymbol{k}_{\text{HOCO}}\sigma\mp\boldsymbol{k}_{\text{HOCO}}\sigma'}\left(H_{\text{applied}}\right)$) with zero kinetic energy (Fig. 3 (b)) become much more stable than the fermionic states ($\psi_{\text{Fermi,IN,}\boldsymbol{k}_{\text{HOCO}}\sigma\boldsymbol{k}'_{\text{HOCO}}\sigma'}\left(H_{\text{applied}}\right)$) with large kinetic energy (Fig. 3 (a)). The bosonic states ($\psi_{\text{Bose,SC,}\pm\boldsymbol{k}_{\text{HOCO}}\sigma\mp\boldsymbol{k}_{\text{HOCO}}\sigma'}\left(H_{\text{applied}}\right)$) are the resonance standing wave states (wave characteristics) composed from the various fermionic traveling wave states ($\psi_{\text{Bose,NM,}\boldsymbol{k}_{\text{HOCO}}\sigma}\left(H_{\text{applied}}\right)$) (observed as particle characteristics). Bosonic and fermionic states are related to the standing wave and traveling waves, respectively.

7. Relationships between the Applied Magnetic Field and Electronic States

7.1 Comparison of the One Bosonic Superconducting Particle States with the Two Fermionic Intrinsic Insulating Particles States

Let us next look into the relationships between the H_{applied} values and the electronic properties in order to investigate the possibility that we can observe two fermionic intrinsic insulating particles states ($\psi_{\text{two,Fermi,IN}}$) (Fig. 3 (a)). When the H_{applied} value increases, and at $H_{\text{applied}} = H_{\text{c,BE}}$, the one bosonic superconducting particle states ($\psi_{\text{two,Bose,SC}}$) (Fig. 3 (b)) would be converted to the two fermionic intrinsic insulating particles states ($\psi_{\text{two,Fermi,IN}}$) (Fig. 3 (a)), theoretically, as follows,

$$\begin{aligned}
&\Delta E_{\text{SC-IN}}\left(H_{\text{c,BE}}\right) \\
&= V_{H_{\text{induced}}}\left(H_{\text{applied}}\right) - 2V_{\text{kin,Fermi},\boldsymbol{k}_{\text{HOCO}}\sigma}\left(H_{\text{c,BE}}\right) \\
&= \frac{\mu_0 H_{\text{c,BE}}^2 v_{\text{SC}}}{2} - 2V_{\text{kin,Fermi},\boldsymbol{k}_{\text{HOCO}}\sigma}\left(H_{\text{c,BE}}\right) \\
&= 0. \qquad (25)
\end{aligned}$$

Therefore, the $H_{\text{c,BE}}$ value can be estimated as

$$H_{\text{c,BE}} = 2\sqrt{\frac{V_{\text{kin,Fermi},\boldsymbol{k}_{\text{HOCO}}\sigma}\left(H_{\text{c,BE}}\right)}{\mu_0 v_{\text{SC}}}}. \qquad (26)$$

The $H_{\text{c,BE}}$ values are very large because of the large $2V_{\text{kin,Fermi},\boldsymbol{k}_{\text{HOCO}}\sigma}\left(H_{\text{c,BE}}\right)$ values of approximately 70 eV, and thus the conversion from the one bosonic superconducting particle states ($\psi_{\text{two,Bose,SC}}$) (Fig. 3 (b)) to the two fermionic intrinsic insulating particles states ($\psi_{\text{two,Fermi,IN}}$) (Fig. 3 (a)) would not be usually realistic.

7.2 Destruction of the One-Bosonic Superconducting Particle States

When the H_{applied} value increases, the one-bosonic superconducting particle states ($\psi_{\text{two,Bose,SC}}$) would be destroyed by the critical field $\min\left(H_{\text{c,singlet}}, H_{\text{c,BE}}\right)$ as follows (Fig. 4). Usually, the $\Delta E_{\text{gap,e-ph}}\left(H_{\text{applied}}\right)$ ($\approx 10^{-2} \sim 10^{-3}$ eV) and $\Delta E_{\text{gap,HOMO-LUMO}}\left(H_{\text{applied}}\right)$ values (≈ 70 eV), and thus the transition from the one-bosonic superconducting particles ($\psi_{\text{two,Bose,SC}}$) to the two one-bosonic normal metallic particles states ($\psi_{\text{one,Bose,NM}}$) occurs before that from the one-bosonic superconducting particle states ($\psi_{\text{two,Bose,SC}}$) to the two-fermionic insulating particles states ($\psi_{\text{two,Fermi,IN}}$) occurs (Fig. 4 (a)). That is, the $H_{\text{c,singlet}}$ value is much smaller than the $H_{\text{c,BE}}$ value. Therefore, the transition from the superconducting states

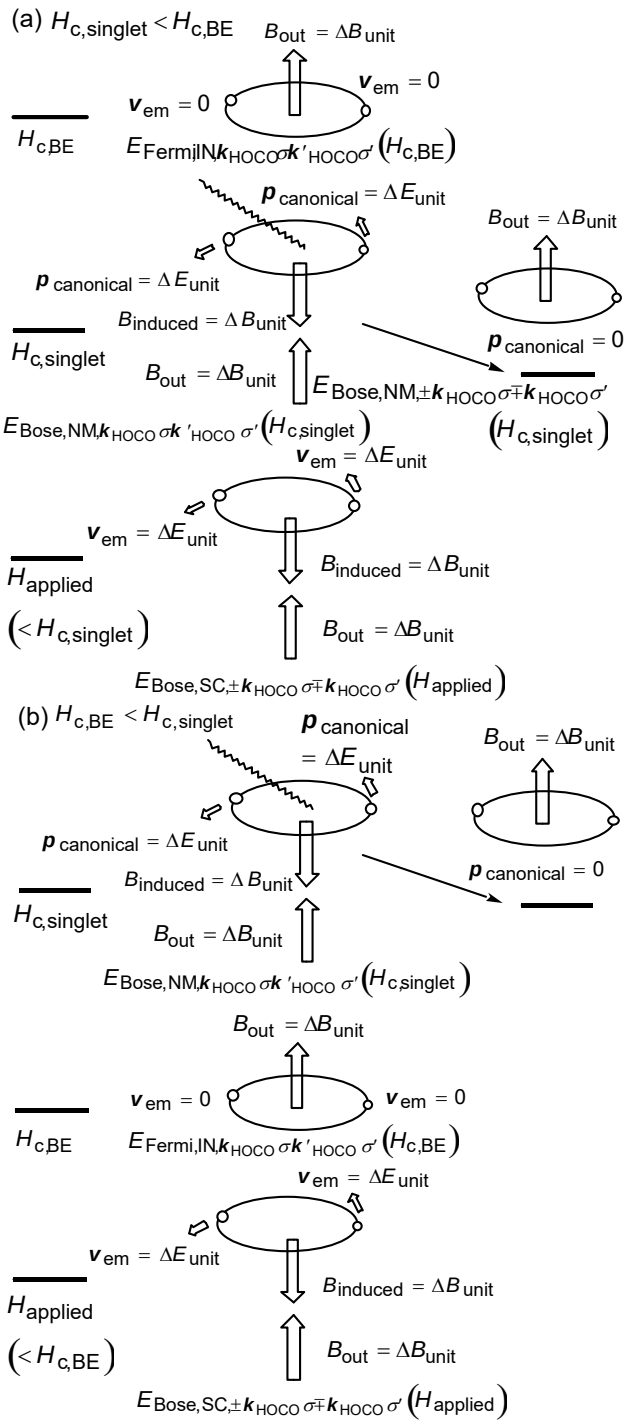

Fig. 4. Destruction of the one-bosonic superconducting particle states. (a) From superconducting state to the normal metallic state. (b) From superconducting state to the insulating state.

($\psi_{\text{two,Bose,SC}}$) to the normal metallic states ($\psi_{\text{one,Bose,NM}}$) can be usually observed at the critical magnetic field $H_{\text{c,singlet}}$ (Fig. 4 (a)). This is the reason

why we usually observe the transition from the superconducting states ($\psi_{\text{two,Bose,SC}}$) to the normal metallic state ($\psi_{\text{one,Bose,NM}}$) and not to the intrinsic insulating states ($\psi_{\text{two,Fermi,IN}}$) (Fig. 4 (a)). On the other hand, if the $\Delta E_{\text{gap,HOMO-LUMO}}\left(H_{\text{applied}}\right)$ values are larger than the $2V_{\text{kin,Fermi},\boldsymbol{k}_{\text{HOCO}}\sigma}\left(H_{\text{applied}}\right)$ values, we can observe the transition from one-bosonic superconducting particle states ($\psi_{\text{two,Bose,SC}}$) to the two-fermionic intrinsic insulating particles states ($\psi_{\text{two,Fermi,IN}}$) at the critical magnetic field $H_{\text{c,BE}}$, theoretically (Fig. 4 (b)). However, even in the neutral He atoms, the $\Delta E_{\text{gap,HOMO-LUMO}}\left(H_{\text{applied}}\right)$ value of 48.2 eV is much smaller than the $2V_{\text{kin,Fermi},\boldsymbol{k}_{\text{HOCO}}\sigma}\left(H_{\text{applied}}\right)$ value of 77.7 eV. Therefore, it would be very difficult to observe the two-fermionic intrinsic insulating particles states ($\psi_{\text{two,Fermi,IN}}$) predicted from the band theory in the textbooks in the conventional solid state physics.

8. New Interpretation of the Spacetime Axis in the Special Relativity

In the previous sections, we suggested the relationships between the superconducting, normal metallic, and insulating states. Related to these relationships, in particular, related to the relationships between the bosonic standing waves and the fermionic traveling waves, and between the non-equilibrium states and the equilibrium states, we will also discuss the relationships between the entropy and the time, in view of the special relativity.

In this article, we define the spacetime components of the particles and antiparticles as follows (Figs. 5 and 6) [19].

The $\boldsymbol{r}_{\boldsymbol{r}_{\text{p}}}$ and $\boldsymbol{r}_{\boldsymbol{r}_{\text{a}}}$ terms denote the real space components at the real 3-dimensional real space axis for particles and antiparticles, respectively. The $\boldsymbol{r}_{\boldsymbol{t}_{\text{p}}}$ and $\boldsymbol{r}_{\boldsymbol{t}_{\text{a}}}$ terms denote the real space components at the real 3-dimensional time axis for particles and antiparticles, respectively.

The $\boldsymbol{t}_{\boldsymbol{t}_{\text{p}}}$ and $\boldsymbol{t}_{\boldsymbol{t}_{\text{a}}}$ terms denote the real time components at the real 1-dimensional time axis for particles and antiparticles, respectively. The $\boldsymbol{t}_{\boldsymbol{r}_{\text{p}}}$ and $\boldsymbol{t}_{\boldsymbol{r}_{\text{a}}}$ terms denote the real time components at the real 1-dimensional space axis for particles and antiparticles, respectively.

The $\boldsymbol{p}_{\boldsymbol{r}_{\text{p}}}$ and $\boldsymbol{p}_{\boldsymbol{r}_{\text{a}}}$ terms denote the real momentum components at the real 3-dimensional space axis for particles and antiparticles, respectively. The $\boldsymbol{p}_{\boldsymbol{t}_{\text{p}}}$ and $\boldsymbol{p}_{\boldsymbol{t}_{\text{a}}}$ terms denote the real momentum components at the real 3-dimensional time axis for particles and antiparticles, respectively.

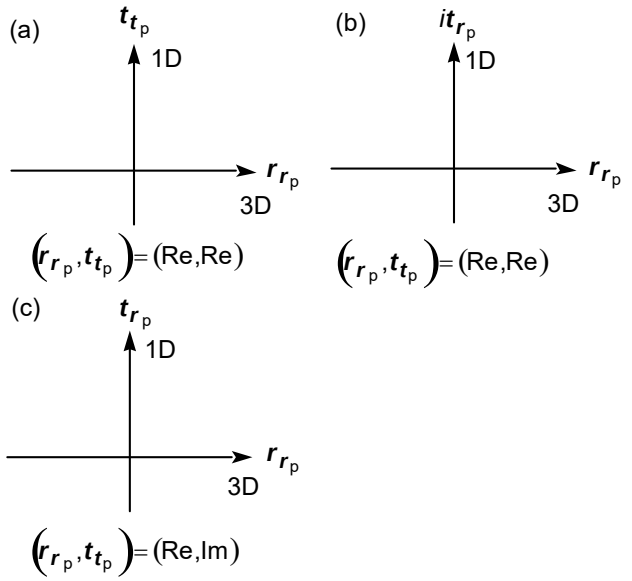

Fig. 5. Relationships between the space and time axes. (a) The 3-dimensional real space axis and the 1-dimensional real time axis. (b) The 3-dimensional real space axis and the 1-dimensional imaginary space axis. (c) The 3-dimensional real space axis and the 1-dimensional real space axis.

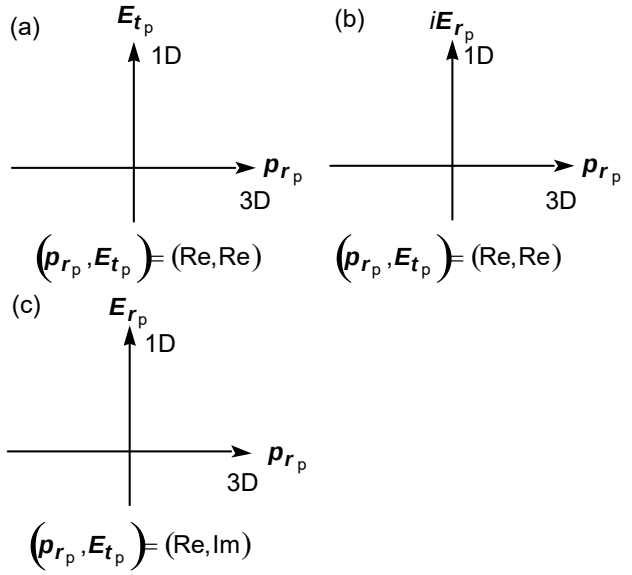

Fig. 6. Relationships between the momentum and energy axes. (a) The 3-dimensional real momentum axis and the 1-dimensional real energy axis. (b) The 3-dimensional real momentum axis and the 1-dimensional imaginary momentum axis. (c) The 3-dimensional real momentum axis and the 1-dimensional real momentum axis.

The $\boldsymbol{E}_{\boldsymbol{t}_p}$ and $\boldsymbol{E}_{\boldsymbol{t}_a}$ terms denote the real energy components at the real 1-dimensional time axis for particles and antiparticles, respectively. The $\boldsymbol{E}_{\boldsymbol{r}_p}$ and $\boldsymbol{E}_{\boldsymbol{r}_a}$ terms denote the real energy components at the real 1-dimensional space axis for particles and antiparticles, respectively.

According to the special relativity and Minkowski's research, the relationships between the space (x, y, z) and time axes (t) can be expressed as

$$x^2 + y^2 + z^2 + (ict)^2 = \text{const.} \quad (27)$$

where the c is the speed of the light.

In other words,

$$\boldsymbol{r}_{\boldsymbol{r}_p}^2 + \left(c\boldsymbol{t}_{\boldsymbol{t}_p}\right)^2 = \text{const.} \quad (28)$$

$$\boldsymbol{r}_{\boldsymbol{r}_a}^2 + \left(c\boldsymbol{t}_{\boldsymbol{t}_a}\right)^2 = \text{const.} \quad (29)$$

On the other hand, the 1-dimensional $\boldsymbol{t}_{\boldsymbol{t}_p}$ and $\boldsymbol{t}_{\boldsymbol{t}_a}$ time vectors, which are real components at the real time axis, are the imaginary components at the real 1-dimensional space axis, as expressed as (Fig. 5 (c)),

$$\boldsymbol{t}_{\boldsymbol{t}_p} = i\boldsymbol{t}_{\boldsymbol{r}_p}, \quad (30)$$

$$\boldsymbol{t}_{\boldsymbol{t}_a} = i\boldsymbol{t}_{\boldsymbol{r}_a}. \quad (31)$$

Therefore,

$$\boldsymbol{r}_{\boldsymbol{r}_p}^2 + \left(c\boldsymbol{t}_{\boldsymbol{t}_p}\right)^2 = \boldsymbol{r}_{\boldsymbol{r}_p}^2 + \left(ic\boldsymbol{t}_{\boldsymbol{r}_p}\right)^2 = \text{const.} \quad (32)$$

$$\boldsymbol{r}_{\boldsymbol{r}_a}^2 + \left(c\boldsymbol{t}_{\boldsymbol{t}_a}\right)^2 = \boldsymbol{r}_{\boldsymbol{r}_a}^2 + \left(ic\boldsymbol{t}_{\boldsymbol{r}_a}\right)^2 = \text{const.} \quad (33)$$

If we consider that we live in the real visible space axis, real time axis ($\boldsymbol{t}_{\boldsymbol{t}_p}$ and $\boldsymbol{t}_{\boldsymbol{t}_a}$) can be considered to be imaginary invisible space axis ($i\boldsymbol{t}_{\boldsymbol{r}_p}$ and $i\boldsymbol{t}_{\boldsymbol{r}_a}$) (Fig. 5 (b)). That is, we can consider that the ct term is related to the real time component (imaginary space component) (Fig. 5 (a)), on the other hand, the ict term is related to the real space component (imaginary time component) (Fig. 5 (b)).

Therefore, we can consider that the real world we live in is the complex 4-dimensional spacetime world which is formed by the real visible 3-dimensional space components (so-called, space axis) and by the imaginary invisible 1-dimensional space component (so-called, time axis), at the real 4-dimensional space axis (Fig. 5 (c)).

The 4-dimensional spacetime axis can be interpreted by various definitions as follows. The components of the 4-dimensional spacetime axis are composed of the 3-dimensional real space vectors at the 3-dimensional real space axis and of the 1-dimensional real time vectors at the 1-dimensional real time axis (Fig. 5 (a)). The components of the 4-dimensional spacetime axis are composed of the 3-dimensional real space vectors at the 3-dimensional real space axis and the 1-dimensional real time vectors at the 1-dimensional imaginary space axis (Fig. 5 (b)). The components of the 4-dimensional spacetime axis are composed of the 3-dimensional real space vectors at the 3-dimensional real space axis and of the 1-dimensional imaginary time vectors at the 1-dimensional real space axis (Fig. 5 (c)). In the discussion in this article, we will use the definition that the components of the 4-dimensional spacetime axis are composed of the 3-dimensional real space vectors at the 3-dimensional real space axis and of the 1-dimensional imaginary time vectors at the 1-dimensional real space axis (Fig. 5 (c)).

From Eqs. (32) and (33), denoting the relationships between the space and time axes, we can derive the equation, denoting the relationships between the momentum (p_x, p_y, p_z, p_t, $p_{t,0}$) and energy (E_x, E_y, E_z, E_t, $E_{t,0}$) by using the mass q_g and the rest mass $q_{g,0}$, as follows (Fig. 6),

$$\left(q_g v_x\right)^2 + \left(q_g v_y\right)^2 + \left(q_g v_z\right)^2 + \left(iq_g c\right)^2 = \left(iq_{g,0} c\right)^2 = \text{const.} < 0, \quad (34)$$

$$p_x^2 + p_y^2 + p_z^2 + p_t^2 = p_{t,0}^2 = \text{const.} < 0, \quad (35)$$

$$p_x^2 + p_y^2 + p_z^2 + \left(\frac{E_t}{c}\right)^2 = \left(\frac{E_{t,0}}{c}\right)^2 = \text{const.} < 0, \quad (36)$$

where

$$p_x = q_g v_x, \quad (37)$$

$$p_y = q_g v_y, \quad (38)$$

$$p_z = q_g v_z, \quad (39)$$

$$p_t = iq_g c, \quad (40)$$

$$p_{t,0} = iq_{g,0} c, \quad (41)$$

$$E_t = cp_t, \quad (42)$$

$$E_{t,0} = cp_{t,0}. \quad (43)$$

In other words (Fig. 6 (a)),

$$p_{r_p}^2 + p_{t_p}^2 = p_{r_p}^2 + \left(\frac{E_{t_p}}{c}\right)^2 = \left(\frac{E_{t_p,0}}{c}\right)^2 = \text{const.} \quad (44)$$

$$p_{r_a}^2 + p_{t_a}^2 = p_{r_a}^2 + \left(\frac{E_{t_a}}{c}\right)^2 = \left(\frac{E_{t_a,0}}{c}\right)^2 = \text{const.} \quad (45)$$

where

$$E_{t_p} = cp_{t_p}, \quad (46)$$

$$E_{t_a} = cp_{t_a}. \quad (47)$$

On the other hand, the 1-dimensional p_{t_p} and p_{t_a} (E_{t_p} and E_{t_a}) momentum (energy) vectors, which are real components at the time axis, are the imaginary components at the real 1-dimensional space axis, as expressed as (Fig. 6 (b), (c)),

$$E_{t_p} = iE_{r_p}, \quad (48)$$

$$E_{t_a} = iE_{r_a}. \quad (49)$$

Therefore, the E_{r_p} and E_{r_a} can be interpreted as the energy momentum vector for the particles and antiparticles, respectively (Fig. 6 (c)). Eq. (36) can be expressed by using vectors as (Fig. 6 (c))

$$p_{r_p}^2 + p_{t_p}^2 = p_{r_p}^2 + \left(\frac{E_{t_p}}{c}\right)^2 = p_{r_p}^2 + \left(\frac{iE_{r_p}}{c}\right)^2 = \left(\frac{iE_{r_p,0}}{c}\right)^2 = \text{const.} \quad (50)$$

$$p_{r_a}^2 + p_{t_a}^2 = p_{r_a}^2 + \left(\frac{E_{t_a}}{c}\right)^2 = p_{r_a}^2 + \left(\frac{iE_{r_a}}{c}\right)^2 = \left(\frac{iE_{r_a,0}}{c}\right)^2 = \text{const.} \quad (51)$$

The momentum p_x, p_y, and p_z values are related to the real components at the real space axis, x, y, and z, respectively. The energy E_t is related to the real (imaginary) component at the real time (real space) axis (Fig. 6 (a)). The p_t and $p_{t,0}$ (E_t / c and $E_{t,0} / c$) terms are usually considered to be related to the energy, that is, related to the real components at the time axis (Fig. 6 (a)). On the other hand, if we consider that we live in the real visible momentum axis, which is related to the real space axis, the energy can be considered to be the imaginary invisible momentum component at the real space axis (Fig. 6 (b), (c)). Therefore, we can consider that the p_t and E_t terms, and the $p_{t,0}$ and $E_{t,0}$ terms, are related to the real time component (imaginary space component), on the other hand, the ip_t and iE_t terms, and the $ip_{t,0}$ and $iE_{t,0}$ terms, are related to the real space component (imaginary time component).

Let us next express the energy components from Eqs. (40) and (41),

$$E_x^2 + E_y^2 + E_z^2 + E_t^2 = E_{t,0}^2 = \text{const.} < 0, \quad (52)$$

$$\sqrt{-\left(E_x^2 + E_y^2 + E_z^2 + E_t^2\right)} = \sqrt{-E_{t,0}^2}, \quad (53)$$

where

$$E_x = cp_x, \quad (54)$$

$$E_y = cp_y, \quad (55)$$

$$E_z = cp_z, \quad (56)$$

$$\sqrt{-\left\{\left(cp_{r_p}\right)^2 + \left(iE_{r_p}\right)^2\right\}} = \sqrt{-\left(iE_{r_p,0}\right)^2}, \quad (57)$$

$$\sqrt{-\left\{\left(cp_{r_a}\right)^2 + \left(iE_{r_a}\right)^2\right\}} = \sqrt{-\left(iE_{r_a,0}\right)^2}, \quad (58)$$

$$\left(cp_{r_p}\right)^2 + \left(iE_{r_p}\right)^2 = \left(iE_{r_p,0}\right)^2, \quad (59)$$

$$\left(cp_{r_a}\right)^2 + \left(iE_{r_a}\right)^2 = \left(iE_{r_a,0}\right)^2. \quad (60)$$

We can see from Eqs. (59) and (60) that the original point ($p_x = p_y = p_z = p_t = 0$) at the spacetime axis in energy is saddle point (massless transition state (TS)) [20] of the converting reaction between massive particle and antiparticle states in momentum-energy curves (Fig. 7).

International Journal of Scientific Engineering and Applied Science (IJSEAS) – Volume-3, Issue-4, April 2017
ISSN: 2395-3470
www.ijseas.com

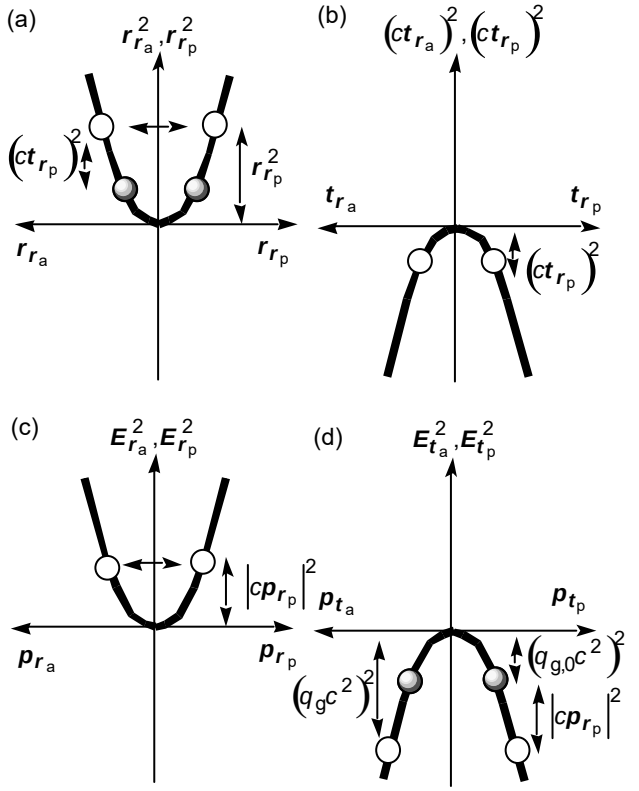

Fig. 7. (a) Scale of the space. The opened and shaded circles indicate the scales of the space and the total spacetime, respectively. (b) Scale of the time denoted by the opened circles. (c) Energy for the space axis denoted by the opened circles. (d) Energy for the time axis. The opened and shaded circles indicate the energies of the time and the total spacetime axes, respectively.

The original point ($p_x = p_y = p_z = p_t = 0$) is the minimum point in energy at the p_x, p_y, and p_z axes ($p_x = p_y = p_z = 0$) (Fig. 7 (a), (c)), on the other hand, that is the maximum point in energy at the real space axis at the p_t axis ($p_t = 0$) (Fig. 7 (d)). Therefore, the space can be considered to be real components (reversible) of the space axis at the spacetime axis (Fig. 7 (c)). On the other hand, the time can be considered to be the imaginary components (irreversible) of the space axis at the spacetime axis (Fig. 7 (d)). That is, the 3-dimensional space components are real components in the real 3-dimensional space axis, and the 1-dimensional time components are the imaginary components in the 1-dimensional real space axis (Fig. 5 (c)).

The original point of the space axis at the spacetime axis is the bottom point, and the most stable in energy (Fig. 7 (c)). Therefore, only small energy is needed for space to reverse at the real space axis. Therefore, the reversible process from the $+\boldsymbol{r}_{\boldsymbol{r}_p}$ to the $-\boldsymbol{r}_{\boldsymbol{r}_p}$ (from the $+\boldsymbol{r}_{\boldsymbol{r}_a}$ to the $-\boldsymbol{r}_{\boldsymbol{r}_a}$) can be possible (Fig. 7 (a), (c)), and we can observe the real space axis, visibly. This is the reason why momentum vectors $\boldsymbol{p}_{\boldsymbol{r}_p}$ and $\boldsymbol{p}_{\boldsymbol{r}_a}$, and related space axis $\boldsymbol{r}_{\boldsymbol{r}_p}$ and $\boldsymbol{r}_{\boldsymbol{r}_a}$, are the 3-dimensional real vectors at the real space axis (Figs. 5 (a) and 6 (a)).

The time can be considered to be the imaginary components (irreversible) of the space axis at the spacetime axis (Fig. 5 (c)). The original point of the time at the real space axis is the top point, and the most unstable in energy (Fig. 7 (b), (d)). Therefore, very large energy is needed for the time to reverse at the real space axis. Therefore, the reversible process from the future $+\boldsymbol{t}_{\boldsymbol{t}_p}$ ($+i\boldsymbol{t}_{\boldsymbol{r}_p}$) to the past $-\boldsymbol{t}_{\boldsymbol{t}_p}$ ($-i\boldsymbol{t}_{\boldsymbol{r}_p}$) (from the future $+\boldsymbol{t}_{\boldsymbol{t}_a}$ ($+i\boldsymbol{t}_{\boldsymbol{r}_a}$) to the past $-\boldsymbol{t}_{\boldsymbol{t}_a}$ ($-i\boldsymbol{t}_{\boldsymbol{r}_a}$)) cannot be possible, furthermore, we cannot observe the real time (imaginary components) at the real space axis, visibly (Fig. 7 (b)). This is the reason why the energy $\boldsymbol{E}_{\boldsymbol{t}_p}$ ($= i\boldsymbol{E}_{\boldsymbol{r}_p}$) and $\boldsymbol{E}_{\boldsymbol{t}_a}$ ($= i\boldsymbol{E}_{\boldsymbol{r}_a}$), and related time axis $\boldsymbol{t}_{\boldsymbol{t}_p}$ ($= i\boldsymbol{t}_{\boldsymbol{r}_p}$) and $\boldsymbol{t}_{\boldsymbol{t}_a}$ ($= i\boldsymbol{t}_{\boldsymbol{r}_a}$), are considered to be not vector but scalar. On the other hand, we can interpret that the energy vectors $\boldsymbol{E}_{\boldsymbol{t}_p}$ ($= i\boldsymbol{E}_{\boldsymbol{r}_p}$) and $\boldsymbol{E}_{\boldsymbol{t}_a}$ ($= i\boldsymbol{E}_{\boldsymbol{r}_a}$), and related time axis $\boldsymbol{t}_{\boldsymbol{t}_p}$ ($= i\boldsymbol{t}_{\boldsymbol{r}_p}$) and $\boldsymbol{t}_{\boldsymbol{t}_a}$ ($= i\boldsymbol{t}_{\boldsymbol{r}_a}$), are the 1-dimensional imaginary vectors at the real space axis (Figs. 5 (c) and 6 (c)).

Particles and antiparticles have intrinsic $\boldsymbol{r}_{\boldsymbol{r}_p} - i\boldsymbol{t}_{\boldsymbol{r}_p}$ and $\boldsymbol{r}_{\boldsymbol{r}_a} - i\boldsymbol{t}_{\boldsymbol{r}_a}$ spacetime axes, respectively. Particles and antiparticles cannot be usually distinguished by each other by reversible space axis ($\boldsymbol{r}_{\boldsymbol{r}_p}$ and $\boldsymbol{p}_{\boldsymbol{r}_p}$, and $\boldsymbol{r}_{\boldsymbol{r}_a}$ and $\boldsymbol{p}_{\boldsymbol{r}_a}$) (Fig. 7 (a), (c)). On the other hand, particles and antiparticles can be usually distinguished by each other by irreversible time axis ($i\boldsymbol{t}_{\boldsymbol{r}_p}$ and $i\boldsymbol{E}_{\boldsymbol{r}_p}$, and $i\boldsymbol{t}_{\boldsymbol{r}_a}$ and $i\boldsymbol{E}_{\boldsymbol{r}_a}$) (Fig. 7 (b), (d)). The dominance of particles rather than antiparticles is the reason why we live only from the past ($-\boldsymbol{t}_{\boldsymbol{t}_p}$ ($-i\boldsymbol{t}_{\boldsymbol{r}_p}$)) to the future ($+\boldsymbol{t}_{\boldsymbol{t}_p}$ ($+i\boldsymbol{t}_{\boldsymbol{r}_p}$)) in the real particle spacetime axis (Fig. 7 (b)).

In summary, the space axis is the real 3-dimensional space vector in the spacetime axis (Fig. 5 (c)). Momentum is the real 3-dimensional momentum vector at the real space axis in the spacetime axis (Fig. 6 (c)). The time is the imaginary 1-dimensional space vector at the real space axis in the spacetime axis (Fig. 5 (c)). The energy is the imaginary 1-dimensional momentum vector at real space axis in the spacetime axis (Fig. 6 (c)).

9. Relationships between the Entropy and Arrow of Time

In the second law of the thermodynamics, it has been described that the direction of the arrow of time should be

International Journal of Scientific Engineering and Applied Science (IJSEAS) – Volume-3, Issue-4, April 2017
ISSN: 2395-3470
www.ijseas.com

defined by the direction of the increase of entropy in the isolated systems. That is, the reason why the direction of the arrow of time should be defined by the direction of the increase of entropy in the isolated systems has not fully been elucidated. Therefore, we will suggest the relationships between the entropy and the time in this section.

9.1 Relationships between the Rest Mass and Stability of the Spacetime in the Microscopic One Particle Systems

Let us next look into the relationships between the rest mass and the stability of the spacetime. As an example, we consider a particle. The relationship between the rest mass energy ($E_{t,0}^2$) and the energy for spacetime ($E_x^2 + E_y^2 + E_z^2 + E_t^2$) can be expressed as

$$E_x^2 + E_y^2 + E_z^2 + E_t^2 = E_{t,0}^2 \le 0, \tag{61}$$

or

$$\boldsymbol{E}_{\boldsymbol{r}_\mathrm{p}}^2 + \boldsymbol{E}_{\boldsymbol{t}_\mathrm{p}}^2 = \boldsymbol{E}_{\boldsymbol{t}_\mathrm{p},0}^2 \le 0, \tag{62}$$

where

$$\boldsymbol{E}_{\boldsymbol{r}_\mathrm{p}}^2 \ge 0, \tag{63}$$

$$\boldsymbol{E}_{\boldsymbol{t}_\mathrm{p}}^2 \le 0, \tag{64}$$

$$\boldsymbol{E}_{\boldsymbol{t}_\mathrm{p},0}^2 \le 0. \tag{65}$$

The $\boldsymbol{E}_{\boldsymbol{t}_\mathrm{p}}$ and $\boldsymbol{E}_{\boldsymbol{t}_\mathrm{p},0}$ values are related to the $\boldsymbol{p}_{\boldsymbol{t}_\mathrm{p}}$ and $\boldsymbol{p}_{\boldsymbol{t}_\mathrm{p},0}$ values, respectively.

The $\boldsymbol{E}_{\boldsymbol{t}_\mathrm{p}}$ value, related to the time flowing velocity $+\Delta\boldsymbol{t}_{\boldsymbol{t}_\mathrm{p}}$, becomes equal to the rest mass energy ($q_{\mathrm{g},0}c^2$) value when the p_x, p_y, and p_z values, related to the space axis, are 0, as follows (Fig. 8 (a)),

$$\lim_{p_x, p_y, p_z \to 0} p_t^2 = p_{t,0}^2 = \left(iq_{\mathrm{g},0}c\right)^2. \tag{66}$$

Therefore, the time flowing velocity $+\Delta\boldsymbol{t}_{\boldsymbol{t}_\mathrm{p}}$ is related to the rest mass $q_{\mathrm{g},0}$ value. Furthermore, the time flowing velocity $+\Delta\boldsymbol{t}_{\boldsymbol{t}_\mathrm{p}}$ is related to the electric charge as well as the rest mass $q_{\mathrm{g},0}$, which are generated as a consequence of the Higgs mechanism.

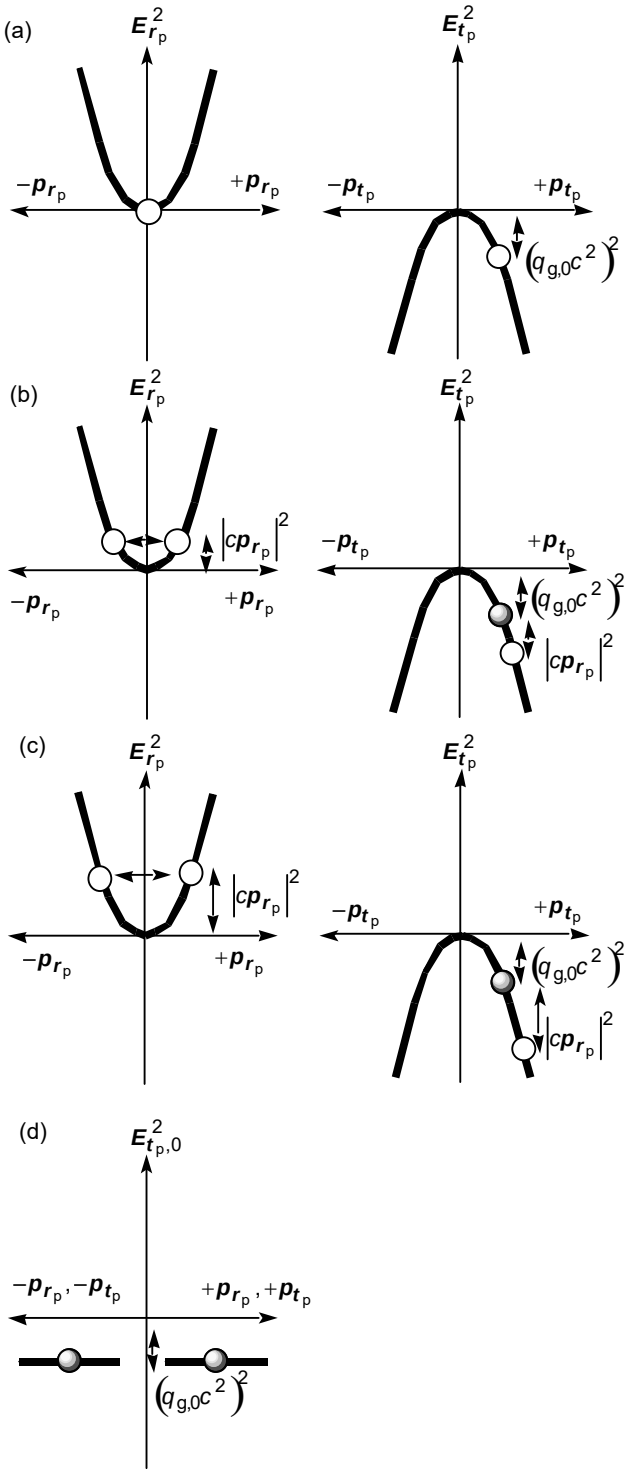

Fig. 8. Energies as a function of the space and time. (a)–(c) Energies for the space and time axes. (d) Total energies for the spacetime axis. In (a)–(d), the opened circles denote the energies for the space and time axes. The shaded circles indicate the total energy for the spacetime axis.

We can see from Eq. (50) that the $|\boldsymbol{p}_{t_p}|$ value increases with an increase in the $|\boldsymbol{p}_{r_p}|$ value. That is, the stabilization energy $|\boldsymbol{E}_{t_p}|$ value increases with an increase in the destabilization energy $|\boldsymbol{E}_{r_p}|$ value so that the total stabilization energy $|\boldsymbol{E}_{t_p,0}|$ value in the spacetime world becomes constant (Fig. 8 (a)–(d)). That is, the total spacetime energy ($|\boldsymbol{E}_{t_p,0}|$) originating from the space axis ($|\boldsymbol{E}_{r_p}|$) and the time axis ($|\boldsymbol{E}_{t_p}|$) try to become always constant by distortion of the spacetime (Fig. 8 (d)). At the same time, the scale of the space $\Delta\boldsymbol{r}_{r_p}$ and the time flowing velocity $\Delta\boldsymbol{t}_{t_p}$ decrease with an increase in the $\boldsymbol{p}_{r_p}$ value. Spacetime becomes very unstable in energy if the $\boldsymbol{p}_{t_p}$ value becomes 0 [19]. That is, the time flowing velocity $\Delta\boldsymbol{t}_{t_p}$ and imaginary momentum vector $\boldsymbol{p}_{t_p}$ at the real space axis (momentum at the time axis), related to the rest mass $q_{g,0}$, play an essential role in the forming of the stable real spacetime world we live in (Fig. 8). Similar discussion can be made in the case of the antiparticles.

Furthermore, the time flowing velocity can be decided by the rest mass $q_{g,0}$ of particle or antiparticle at $p_x = p_y = p_z = 0$. The rest mass $q_{g,0}$ of particle and antiparticle plays an essential role in the forming of the stable spacetime world for particles and antiparticles, respectively (Fig. 8 (d)). The stabilization energy for the spacetime increases with an increase in the rest mass $q_{g,0}$ (Fig. 8).

Let us next consider the second law of the thermodynamics. The free energy such as Gibbs free energy G can be expressed as

$$G = H - TS, \tag{67}$$

$$\Delta G = \Delta H - T\Delta S, \tag{68}$$

where the H, T, and S values denote the enthalpy, temperature, and entropy, respectively.

Let us consider the relationships between the second law of the thermodynamics (Eqs. (67) and (68)) and the special relativity (Eq. (59)). Eq. (59) can be re-expressed as

$$\left(c\boldsymbol{p}_{r_p}\right)^2 = \boldsymbol{E}_{r_p}^2 - \boldsymbol{E}_{r_p,0}^2. \tag{69}$$

$$\Delta\left(c\boldsymbol{p}_{r_p}\right)^2 = \Delta\boldsymbol{E}_{r_p}^2 - \Delta\boldsymbol{E}_{r_p,0}^2. \tag{70}$$

In view of Eqs. (67), and (69), we can consider that the momentum energy $\left(c\boldsymbol{p}_{r_p}\right)^2$, the time momentum energy $\boldsymbol{E}_{r_p}^2$, and the rest mass energy $\boldsymbol{E}_{r_p,0}^2$ in the special relativity, can be related to the (Gibbs) free energy G, the enthalpy H, and the entropy S in the second law of the thermodynamics, respectively,

$$c\boldsymbol{p}_{r_p} \leftrightarrow G, \tag{71}$$

$$\boldsymbol{E}_{r_p} \leftrightarrow H, \tag{72}$$

$$\boldsymbol{E}_{r_p,0} \leftrightarrow TS. \tag{73}$$

Let us consider a particle in the isolated systems even though Eqs. (67) and (68) can be usually used statistically in the macroscopic many particles systems (Fig. 9 (a)). In such a case, one particle moves in whole space in the isolated systems at the constant speed in various direction, and thus we can consider that the $\Delta\left(c\boldsymbol{p}_{r_p}\right)^2$ and $\Delta\boldsymbol{E}_{r_p}^2$ values in the special relativity, and the ΔG and ΔH values in the second law of the thermodynamics, are 0, as shown in Fig. 9 (a).

$$\Delta\left(c\boldsymbol{p}_{r_p}\right)^2 = 0, \tag{74}$$

$$\Delta G = 0, \tag{75}$$

$$\Delta\boldsymbol{E}_{r_p}^2 = 0, \tag{76}$$

$$\Delta H = 0. \tag{77}$$

Therefore, we can consider the change of entropy (ΔS) as follows,

$$\Delta\boldsymbol{E}_{r_p,0}^2 = 0, \tag{78}$$

$$\Delta S = \frac{\Delta H - \Delta G}{T} = 0. \tag{79}$$

Therefore, we can consider that the entropy S does not change with an increase in time ($+\Delta\boldsymbol{t}_{t_p}$) ($\Delta S = 0$) even when one particle moves around within an isolated system. At the same time, the rest mass $q_{g,0}$ and $\boldsymbol{E}_{r_p,0}^2$ values do not change with an increase in time, as

expected, according to the special relativity, as described above. That is, we can conclude that the time flowing velocity $+\Delta t_{t_p}$ does not change when the entropy S does not change. Furthermore, we should also notice that the scale of the space $+\Delta r_{r_p}$ also does not change with an increase in time $+\Delta t_{t_p}$ under the constant velocity moving. The zero value of the change of the entropy ($\Delta S = 0$) and the Gibbs free energy ($\Delta G = 0$) in the second law of the thermodynamics, and the zero value of the change of the $\left(cp_{r_p}\right)^2$ ($\Delta\left(cp_{r_p}\right)^2 = 0$) and $E^2_{r_p,0}$ ($\Delta E^2_{r_p,0} = 0$) values in the special relativity, are the main reason why one particle moving can be considered to be reversible even at the isolated systems, and furthermore, is the reason why the reversible process can be generally applied in the classical dynamics in which each material can be treated. On the other hand, it should be noted that the average momentum p_{r_p} for even one particle should be 0 if we observe one particle for a long time.

9.2 Relationships between the Rest Mass and Stability of the Spacetime in the Macroscopic Many Particles Systems

Let us consider many particles such as molecules, atoms, quarks, leptons, photons, and phonons (heats), and so on, in the macroscopic isolated systems by considering Eqs. (67)–(70). We consider that all particles locate at the only left side of the isolated systems at the beginning (Fig. 9 (b)). By considering Eq. (70), we define the change of the momentum energy $\Delta\left(cp_{r_p,\text{macro}}\right)^2$, the time momentum energy $\Delta E^2_{r_p,\text{macro}}$, and the rest mass energy $\Delta E^2_{r_p,0,\text{macro}}$ in the macroscopic isolated systems in the special relativity, as follows,

$$\Delta\left(cp_{r_p,\text{macro}}\right)^2 = \Delta E^2_{r_p,\text{macro}} - \Delta E^2_{r_p,0,\text{macro}}. \qquad (80)$$

The $E_{r_p,0,\text{macro}}$ value can be expressed by using the effective total mass $q_{g,0,\text{macro}}$ of all particles in the macroscopic isolated systems as

$$E_{r_p,0,\text{macro}} = q_{g,0,\text{macro}}c^2. \qquad (81)$$

As an example, we schematically show the p_{r_p} value around the center of the macroscopic isolated many particles systems (Fig. 9 (b)). Similar discussions can be made in the another all regions in the macroscopic isolated many particles system under consideration. In order to consider the total $p_{r_p,\text{macro}}$ value in the whole isolated

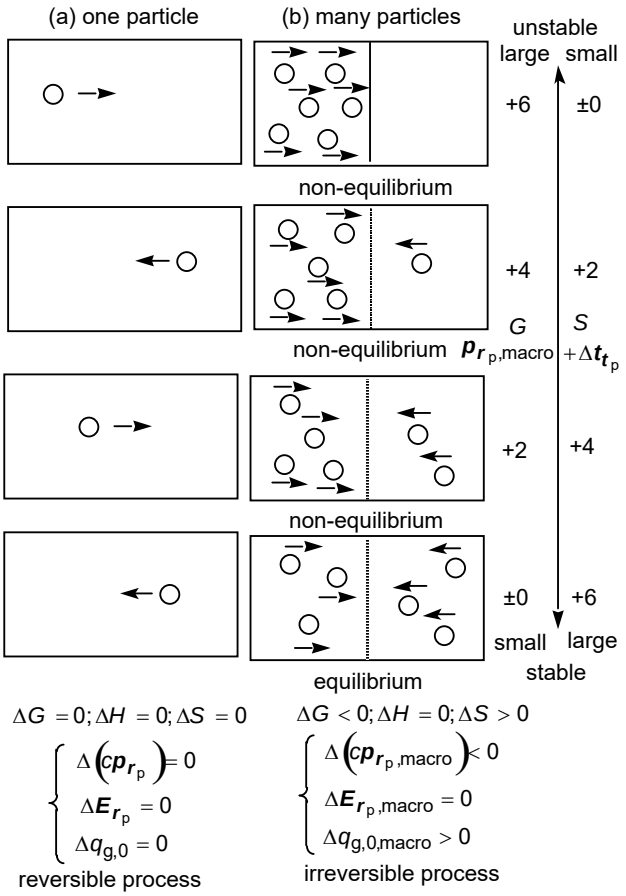

Fig. 9. Relationships between the entropy change and time flowing velocity. (a) One particle system. (b) Many particles system.

macroscopic many particles systems, we should consider the total effects originating from the every partial region in the whole of the isolated many particles system. When the wall located at the center of the isolated systems is removed, many particles can start to move in whole space in the macroscopic isolated systems at various speeds towards various directions (Fig. 9 (b)). In the isolated systems, we can consider that the $\Delta E^2_{r_p,\text{macro}}$ values in the special relativity and the ΔH values in the second law of the thermodynamics, are constant, 0, with an increase in the reaction time ($+\Delta t_{t_p}$) (Fig. 9 (b)). The total velocity originating from all particles in the macroscopic isolated systems decrease with an increase in the reaction time ($+\Delta t_{t_p}$) from the non-equilibrium state to the equilibrium state. Therefore, the $\left(cp_{r_p,\text{macro}}\right)^2$ values in the special relativity and the ΔG values in the second law of the

thermodynamics decrease with an increase in the reaction time ($+\Delta \boldsymbol{t}_{\mathrm{t_p}}$) from the non-equilibrium state to the equilibrium state, as shown in Fig. 9 (b).

$$\Delta\left(c\boldsymbol{p}_{\boldsymbol{r}_{\mathrm{p}},\mathrm{macro}}\right)^2 < 0, \tag{82}$$

$$\Delta G < 0, \tag{83}$$

$$\Delta \boldsymbol{E}^2_{\boldsymbol{r}_{\mathrm{p}},\mathrm{macro}} = 0, \tag{84}$$

$$\Delta H = 0. \tag{85}$$

Therefore, we can consider the change of entropy (ΔS) as follows,

$$\Delta \boldsymbol{E}^2_{\boldsymbol{r}_{\mathrm{p}},0,\mathrm{macro}} > 0, \tag{86}$$

$$\Delta S = \frac{\Delta H - \Delta G}{T} > 0. \tag{87}$$

Therefore, we can consider that the entropy S increases with an increase in the reaction time ($+\Delta \boldsymbol{t}_{\mathrm{t_p}}$) ($\Delta S > 0$) when many particles move towards various directions within an isolated system. At the same time, the effective total mass $q_{\mathrm{g},0,\mathrm{macro}}$ of all particles in the macroscopic isolated systems and $\Delta \boldsymbol{E}^2_{\boldsymbol{r}_{\mathrm{p}},0,\mathrm{macro}}$ values increase with an increase in the reaction time ($+\Delta \boldsymbol{t}_{\mathrm{t_p}}$), as expected, according to the special relativity, as described above. That is, we can conclude that the time flowing velocity $+\Delta \boldsymbol{t}_{\mathrm{t_p}}$ increases with an increase in the entropy S. Furthermore, we should also notice that the scale of the space $+\Delta \boldsymbol{r}_{\mathrm{p}}$ also becomes larger with an increase in the entropy S and the reaction time ($+\Delta \boldsymbol{t}_{\mathrm{t_p}}$). Spacetime becomes stabilized by the increasing nonzero value of the entropy ($\Delta S > 0$) and the decreasing nonzero value of the Gibbs free energy ($\Delta G < 0$) in the second law of the thermodynamics, and by the increase nonzero value of the isolated macroscopic rest mass energy ($\Delta \boldsymbol{E}^2_{\boldsymbol{r}_{\mathrm{p}},0,\mathrm{macro}} > 0$) and the decreasing nonzero value of the total momentum of the isolated macroscopic many particles system ($\Delta\left(c\boldsymbol{p}_{\boldsymbol{r}_{\mathrm{p}}}\right)^2 < 0$) in the special relativity. Therefore, the increasing nonzero value of the entropy ($\Delta S > 0$) and the decreasing nonzero value of the Gibbs free energy ($\Delta G < 0$) in the second law of the thermodynamics, and the increase nonzero value of the isolated macroscopic rest mass energy ($\Delta \boldsymbol{E}^2_{\boldsymbol{r}_{\mathrm{p}},0,\mathrm{macro}} > 0$) and the decreasing nonzero value of the total momentum of the isolated macroscopic many particles system ($\Delta\left(c\boldsymbol{p}_{\boldsymbol{r}_{\mathrm{p}}}\right)^2 < 0$) in the special relativity, are the main reason why many particles moving can be considered to be statistically irreversible in the macroscopic isolated systems, even though each one particle moving can be considered to be reversible in the isolated systems, and the reversible process can be applied in the classical dynamics in which each material can be treated.

It should be noted that the entropy S for each one particle does not change with an increase in the reaction time ($+\Delta \boldsymbol{t}_{\mathrm{t_p}}$) ($\Delta S = 0$) even when one particle moves around within the isolated many particles system. At the same time, the rest mass $q_{\mathrm{g},0}$ and $\boldsymbol{E}^2_{\boldsymbol{r}_{\mathrm{p}},0}$ values for each one particle do not change with an increase in the reaction time, as expected, according to the special relativity. On the other hand, the $\left(c\boldsymbol{p}_{\boldsymbol{r}_{\mathrm{p}},\mathrm{macro}}\right)^2$ and G values decrease, and the $\boldsymbol{E}_{\boldsymbol{r}_{\mathrm{p}},0,\mathrm{macro}}$ ($= q_{\mathrm{g},0,\mathrm{macro}}c^2$) and S values increase, with an increase in the reaction time ($+\Delta \boldsymbol{t}_{\mathrm{t_p}}$) in the macroscopic isolated many particles system as a whole. That is, the total $\left(c\boldsymbol{p}_{\boldsymbol{r}_{\mathrm{p}},\mathrm{macro}}\right)^2$ and G values in the whole space of the isolated many particles systems, which are summation of the $\left(c\boldsymbol{p}_{\boldsymbol{r}_{\mathrm{p}}}\right)^2$ and G values for every space, decrease with an increase in the reaction time ($+\Delta \boldsymbol{t}_{\mathrm{t_p}}$) (Fig. 9 (b)). Therefore, there is a possibility that the stabilization of the spacetime in the isolated many particles systems as a whole originating from the decrease of the $\left(c\boldsymbol{p}_{\boldsymbol{r}_{\mathrm{p}},\mathrm{macro}}\right)^2$ and G values, and originating from the increase of the $\Delta \boldsymbol{E}^2_{\boldsymbol{r}_{\mathrm{p}},0,\mathrm{macro}}$ and S values, according to the special relativity, are related to the seeds of the irreversible process, and related to the driving force of the behavior of many particles as a whole statistically obeying the molecular chaos hypothesis in the Boltzmann's statistical theory. We can consider that the second law of the thermodynamics (increase of the entropy) means that the time flowing velocity $+\Delta \boldsymbol{t}_{\mathrm{t_p}}$ tries to become as large as possible in the spacetime world we live, according to the macroscopic rest mass $q_{\mathrm{g},0,\mathrm{macro}}$ value, and that the spacetime we live in becomes as stable as possible, according to the macroscopic rest mass $q_{\mathrm{g},0,\mathrm{macro}}$ value. The possible maximum time flowing velocity $+\Delta \boldsymbol{t}_{\mathrm{t_p},\mathrm{max}}$ value can be decided by the distortion of the spacetime axis and the rest mass $q_{\mathrm{g},0,\mathrm{macro}}$. The time flowing velocity $+\Delta \boldsymbol{t}_{\mathrm{t_p}}$ value tries to become larger with an

increase in the entropy S, and finally become the $+\Delta \boldsymbol{t}_{t_{\mathrm{p}},\max}$ value, according to the $q_{\mathrm{g},0,\mathrm{macro}}$ value in the special relativity and the maximum entropy $S_{\max}$ value in the second law of the thermodynamics. Furthermore, we can consider that the spacetime world we live in becomes stabilized with an increase in the entropy because the Gibbs free energy (G) is converted to the potential macroscopic rest mass energy ($q_{\mathrm{g},0,\mathrm{macro}}c^2$) in the whole of the isolated many particles system. In other words, there is a possibility that the spacetime world we live in becomes more stable with an increase in the above conversion and the entropy, and this is the reason why we observe the second law of the thermodynamics.

9.3 The New Interpretation of the Relationships between the Entropy and the Arrow of the Time

Let us next discuss the new interpretation of the relationships between the entropy and the arrow of the time. In the second law of thermodynamics, it has been considered that the direction of the arrow of time should be defined by the direction of the increase of entropy in the isolated systems. On the other hand, according to our research results, on the basis of the special relativity, it should be considered that the time irreversibly flows only from the past to the future at the particle time axis because the particles with the time momentum vectors flowing from the past to the future at the particle time axis are more dominant than antiparticles with the time momentum vector flowing from the past to the future at the antiparticle time axis (from the future to the past at the particle time axis) in the real spacetime world we live. That is, the time flows always from the past to the future even when the reaction can artificially occur so that the entropy decreases with an increase in the reaction time [19]. The time flowing velocity $+\Delta \boldsymbol{t}_{t_{\mathrm{p}}}$ decreases with a decrease in the entropy S. Therefore, the second law of the thermodynamics is not directly related to the direction of the arrow of the time itself.

In summary, regardless of the second law of the thermodynamics, we can conclude without any assumption that the time always irreversibly flows only from the past to the future at the particle time axis because the particles with the time momentum vectors flowing from the past to the future at the particle time axis are more dominant than antiparticles with the time momentum vector flowing from the past to the future at the antiparticle time axis (from the future to the past at the particle time axis) in the real spacetime world we live [19].

Let us next look into the relationships between the entropy and the time flowing velocity. We can consider that the entropy increases with an increase in the reaction time when many particles such as quarks, leptons, photons, and phonons (heats) move towards various directions within an isolated system. At the same time, the effective total mass $q_{\mathrm{g},0,\mathrm{macro}}$ of all particles in the macroscopic isolated systems increases with an increase in the reaction time, according to the special relativity. We can conclude that the time flowing velocity increases with an increase in the entropy. Furthermore, we should also notice that the scale of the space also becomes larger with an increase in the entropy and time. The increasing nonzero value of the entropy ($\Delta S > 0$) and the decreasing nonzero value of the Gibbs free energy ($\Delta G < 0$) in the second law of the thermodynamics, and the increase nonzero value of the isolated macroscopic rest mass energy ($\Delta \boldsymbol{E}^2_{\boldsymbol{r}_{\mathrm{p}},0,\mathrm{macro}} > 0$) and the decreasing nonzero value of the total momentum of the isolated macroscopic many particles system ($\Delta\left(c\boldsymbol{p}_{\boldsymbol{r}_{\mathrm{p}},\mathrm{macro}}\right)^2 < 0$) in the special relativity, are the main reason why many particles moving can be considered to be statistically irreversible in the macroscopic isolated systems, even though each one particle moving can be considered to be reversible in the isolated systems, and the reversible process can be applied in the classical dynamics in which each material can be treated.

Let us reconsider the meaning of the second law of the thermodynamics, that is, of the increasing of entropy in the isolated systems. In the isolated systems, the $\Delta \boldsymbol{E}^2_{\boldsymbol{r}_{\mathrm{p}},\mathrm{macro}}$ values in the special relativity and the ΔH values in the second law of the thermodynamics are 0. On the other hand, the $\left(c\boldsymbol{p}_{\boldsymbol{r}_{\mathrm{p}}}\right)^2$ values in the special relativity and the G values in the second law of the thermodynamics decrease with an increase in the reaction time from the non-equilibrium state to the equilibrium state. At the same time, the entropy S in the second law of the thermodynamics and the $\boldsymbol{E}^2_{\boldsymbol{r}_{\mathrm{p}},0,\mathrm{macro}}\left(=q_{\mathrm{g},0,\mathrm{macro}}c^2\right)^2$ values in the special relativity increase with an increase in the reaction time when many particles move towards various directions within an isolated system. The entropy S and the isolated macroscopic rest mass energy $\boldsymbol{E}^2_{\boldsymbol{r}_{\mathrm{p}},0,\mathrm{macro}}\left(=q_{\mathrm{g},0,\mathrm{macro}}c^2\right)^2$ increase with a decrease in the free energy such as the Gibbs free energy G and the isolated macroscopic total momentum $\left(c\boldsymbol{p}_{\boldsymbol{r}_{\mathrm{p}},\mathrm{macro}}\right)^2$, and thus the spacetime world becomes stabilized. That is, we can consider that the entropy S and the isolated macroscopic rest mass energy $\boldsymbol{E}^2_{\boldsymbol{r}_{\mathrm{p}},0,\mathrm{macro}}\left(=q_{\mathrm{g},0,\mathrm{macro}}c^2\right)^2$ increases with an increase in

the reaction time so that the spacetime world in the isolated system can be more stable by decreasing the free energy such as the Gibbs free energy G and the isolated macroscopic total momentum $\left(c\boldsymbol{p}_{\boldsymbol{r}_{\mathrm{p}},\mathrm{macro}}\right)^2$. At the same time, the scale of the space and the time flowing velocity increase with an increase in entropy S and the isolated macroscopic rest mass energy $\boldsymbol{E}^2_{\boldsymbol{r}_{\mathrm{p}},0,\mathrm{macro}}\left(=q_{\mathrm{g},0,\mathrm{macro}}c^2\right)^2$. On the other hand, the scale of the space and the time flowing velocity decrease with a decrease in the entropy S and the isolated macroscopic rest mass energy $\boldsymbol{E}^2_{\boldsymbol{r}_{\mathrm{p}},0,\mathrm{macro}}\left(=q_{\mathrm{g},0,\mathrm{macro}}c^2\right)^2$.

In summary, the change of the entropy is closely related to the time flowing velocity but not directly related to the direction of the arrow of the time itself. The increase of the entropy in the isolated systems play an essential role in the stabilization of the spacetime world by decreasing the free energy such as the Gibbs free energy G and the isolated macroscopic total momentum $\left(c\boldsymbol{p}_{\boldsymbol{r}_{\mathrm{p}},\mathrm{macro}}\right)^2$, in the enlargement of the scale of the space world, in the increase of the time flowing velocity, and in the enlargement of the macroscopic isolated total rest mass $q_{\mathrm{g},0,\mathrm{macro}}$ in many particles system.

The entropy for the fermionic traveling electronic wave, related to the non-equilibrium state, is smaller than that for the bosonic standing electronic wave, related to the equilibrium state. This is the reason why the fermionic traveling electronic wave, related to the non-equilibrium state, is less stable than the bosonic standing electronic wave, related to the equilibrium state.

10. Concluding remarks

In this research, we show the reason why the Meissner effect can be observed in superconductivity. The electronic structures in superconductivity are very similar to those in the insulating states in that they have large $\Delta E_{\mathrm{HOMO-LUMO},N}$ value (more than a few eV), and their valence bands are completely occupied by electrons. On the basis of these results, we suggest that the nondissipative currents observed at room temperatures in the microscopic sized materials as well as the superconducting currents in the macroscopic sized superconductivity can be formed by Cooper pairs. That is, we show that the nondissipative currents observed at room temperatures in the microscopic sized materials can be considered as superconductivity.

We reconsidered the interpretation of the BCS theory. According to the BCS theory, we consider that two fermionic electrons are condensated into one bosonic Cooper pair as a consequence of electron–phonon interactions, and at the same time, the Bose–Einstein condensation occurs. On the other hand, according to our research, the $\Delta E_{\mathrm{gap,NM-SC}}(0)$ and $\Delta E_{\mathrm{gap,e-ph}}(0)$ values appearing in the BCS theory do not denote the Bose–Einstein condensation energy but denote the stabilization energy of the two fermionic electrons in the closed-shell electronic structure after electron–phonon interactions ($E_{\mathrm{Fermi},\boldsymbol{k}_{\mathrm{HOCO}}\sigma\boldsymbol{k}'_{\mathrm{HOCO}}\sigma',\mathrm{after}}(0)$) with respect to the two fermionic electrons in the opened-shell electronic structure before electron–phonon interactions ($E_{\mathrm{Fermi},\boldsymbol{k}_{\mathrm{HOCO}}\sigma\boldsymbol{k}'_{\mathrm{HOCO}}\sigma',\mathrm{before}}(0)$). We should consider that after electron–phonon interactions are completed ($E_{\mathrm{Fermi},\boldsymbol{k}_{\mathrm{HOCO}}\sigma\boldsymbol{k}'_{\mathrm{HOCO}}\sigma',\mathrm{after}}(0)$), the Bose–Einstein condensation can occur ($E_{\mathrm{Bose},\pm\boldsymbol{k}_{\mathrm{HOCO}}\sigma\mp\boldsymbol{k}_{\mathrm{HOCO}}\sigma',\mathrm{after}}(0)$), in the BCS theory. In such a case, the Bose–Einstein condensation energy ($\Delta E_{\mathrm{BE},\boldsymbol{k}_{\mathrm{HOCO}}\sigma\boldsymbol{k}'_{\mathrm{HOCO}}\sigma'}(0)$) denotes the stabilization energy of a bosonic Cooper pair in the closed-shell electronic structure after the electron–phonon interactions ($E_{\mathrm{Bose},\pm\boldsymbol{k}_{\mathrm{HOCO}}\sigma\mp\boldsymbol{k}_{\mathrm{HOCO}}\sigma',\mathrm{after}}(0)$) with respect to the two fermionic electrons in the closed-shell electronic structure after the electron–phonon interactions ($E_{\mathrm{Fermi},\boldsymbol{k}_{\mathrm{HOCO}}\sigma\boldsymbol{k}'_{\mathrm{HOCO}}\sigma',\mathrm{after}}(0)$). In the Meissner effect, the electric and magnetic fields can be induced because the initial ground electronic state tries not to receive the applied external magnetic field, as much as possible, in order that the electronic state does not change from the initial ground electronic state. This expulsion originates from very stable bosonic standing wave state (70 eV) with zero momentum formed by two components of the fermionic traveling waves of two electrons with opposite momentum and spins.

In the closed-shell electronic structure in superconductivity, two electrons occupying the same orbital j have the opposite momentum and spins ($\left|+\boldsymbol{k}_j\uparrow,-\boldsymbol{k}_j\downarrow\right\rangle$ and $\left|+\boldsymbol{k}_j\downarrow,-\boldsymbol{k}_j\uparrow\right\rangle$) by each other, and are condensated into the zero-momentum state (Bose–Einstein condensation), and therefore, there is the bosonic standing wave ($\left|\boldsymbol{k}_{\mathrm{ground,two}}\right\rangle$) with zero momentum ($\boldsymbol{p}_{\mathrm{canonical}}=0$) formed by two fermionic electrons. Since each fermionic electron ($\left|+\boldsymbol{k}_j\uparrow\right\rangle$ and $\left|-\boldsymbol{k}_j\downarrow\right\rangle$, and $\left|+\boldsymbol{k}_j\downarrow\right\rangle$ and $\left|-\boldsymbol{k}_j\uparrow\right\rangle$) has the kinetic energy of about 35 eV, the condensation energy for two electrons ($\left|\boldsymbol{k}_{\mathrm{ground,two}}\right\rangle$) ($\boldsymbol{p}_{\mathrm{canonical}}=0$) is very large, and usually is about 70 eV. This bosonic standing wave state ($\left|\boldsymbol{k}_{\mathrm{ground,two}}\right\rangle$), related to the Cooper pair in superconductivity, is very rigid and stable because of the

closed-shell electronic structure in the two-electrons systems ($\left|+\boldsymbol{k}_j\uparrow,-\boldsymbol{k}_j\downarrow\right\rangle$ and $\left|+\boldsymbol{k}_j\downarrow,-\boldsymbol{k}_j\uparrow\right\rangle$). This is closely related to the condensation of electrons into the zero momentum state ($\boldsymbol{p}_{\text{canonical}}=0$) in the one-electron system in the London theory in superconductivity.

Related to these relationships, in particular, related to the relationships between the bosonic standing waves and the fermionic traveling waves, and between the non-equilibrium states and the equilibrium states, we also discussed the relationships between the entropy and the time.

Acknowledgments

This work is supported by The Iwatani Naoji Foundation's Research Grant.

References

[1] T. Kato, "Diamagnetic currents in the closed-shell electronic structures in sp^3-type hydrocarbons" Chemical Physics, vol. 345, 2008, pp. 1–13.
[2] T. Kato, "The essential role of vibronic interactions in electron pairing in the micro- and macroscopic sized materials" Chemical Physics, vol. 376, 2010, pp. 84–93.
[3] T. Kato, "The role of phonon- and photon-coupled interactions in electron pairing in solid state materials" Synthetic Metals, vol. 161, 2011, pp. 2113–2123.
[4] T. Kato, "New Interpretation of the role of electron-phonon interactions in electron pairing in superconductivity" Synthetic Metals, vol. 181, 2013, pp. 45–51.
[5] T. Kato, "Relationships between the intrinsic properties of electrical currents and temperatures" Proceedings of Eleventh TheIIER International Conference, February 2015, Singapore, pp. 63–68.
[6] T. Kato, "Relationships between the nondissipative diamagnetic currents in the microscopic sized atoms and molecules and the superconductivity in the macroscopic sized solids" Proceedings of Eleventh TheIIER International Conference, February 2015, Singapore, pp. 69–80.
[7] T. Kato, "Vibronic stabilization under the external applied fields" Proceedings of Eleventh TheIIER International Conference, February 2015, Singapore, pp. 110–115.
[8] T. Kato, K. Yoshizawa, and K. Hirao, "Electron-phonon coupling in negatively charged acene- and phenanthrene-edge-type hydrocarbons" J. Chem. Phys. vol. 116, 2002, pp. 3420-3429.
[9] R. Mitsuhashi, Y. Suzuki, Y. Yamanari, H. Mitamura, T. Kambe, N. Ikeda, H. Okamoto, A. Fujiwara, M. Yamaji, N. Kawasaki, Y. Maniwa, and Y. Kubozono, "Superconductivity in alkali-metal-doped picene" Nature vol. 464, 2010, pp. 76-79.
[10] T. Kato, "Electronic Properties under the External Applied Magnetic Field in the Normal Metallic and Superconducting States" Int. J. Sci. Eng. Appl. Sci., vol. 1, Issue 7, 2015, pp.300-320.
[11] T. Kato, "Electron–Phonon Interactions under the External Applied Electric Fields in the Normal Metallic and Superconducting States in Various Sized Materials" Int. J. Sci. Eng. Appl. Sci., vol. 1, Issue 8, 2015, pp.1-16.
[12] M. Murakami, Chodendo Shin-Jidai (meaning "New Era for Research of Superconductivity"), Kogyo-Chosa-kai, Tokyo, 2001 (in Japanese).
[13] T. Kato, "Relationships between the Electric and Magnetic Fields" Int. J. Sci. Eng. Appl. Sci., vol. 1, Issue 9, 2015, pp.128-139.
[14] T. Kato, "Unified Interpretation of the Gravitational, Electric, Magnetic, and Electromagnetic Forces" Int. J. Sci. Eng. Appl. Sci., vol. 2, Issue 1, 2016, pp.153-165.
[15] T. Kato, "Relationships between the Electromagnetic and Strong Forces" Int. J. Sci. Eng. Appl. Sci., vol. 2, Issue 2, 2016, pp.119-134.
[16] T. Kato, "Higgs Mechanism in Superconductivity and Weak Interactions" Int. J. Sci. Eng. Appl. Sci., vol. 2, Issue 3, 2016, pp.148-170.
[17] S. Asai, Higgs-Ryushi No Nazo (meaning "Mystery of Higgs Particle"), Shoden-Sha, Tokyo, 2012 (in Japanese).
[18] T. Kato, "Relationships between the Electric Charges and the Matters and Antimatters" Int. J. Sci. Eng. Appl. Sci., vol. 2, Issue 12, 2016, pp.143-172.
[19] T. Kato, "The Mechanism of the Particle–Antiparticle Pair Annihilation" Int. J. Sci. Eng. Appl. Sci., vol. 3, Issue 3, 2017, pp.7-21.
[20] T. Kato, S.-Y. Kang, X. Xu, and T. Yamabe "Possible Dissociative Adsorption of CH_3OH and CH_3NH_2 on Si(100)-2×1 Surface" J. Phys. Chem. B, vol. 105, 2001, pp. 10340–10347.

Author Profile

Dr. Takashi Kato is a Professor at Nagasaki Institute of Applied Science, Japan. He completed his doctorate in physical chemistry with the theory of vibronic interactions and Jahn–Teller effects at Kyoto University (PhD (Engineering)), Japan, in 2000. During October 2001-February 2003, he has performed research concerning prediction of the occurrence of superconductivity of graphene-like aromatic hydrocarbons such as phenanthrene, picene, and coronene at Max-Planck-Institute for Solid State Research in Stuttgart, Germany, as a visiting scientist. In 2010, his prediction of the occurrence of superconductivity of picene and coronene were experimentally confirmed at Okayama University, Japan, and in 2011, that of phenanthrene was experimentally confirmed at University of Science and

Technology of China. His theory and calculations concerning the guiding principle towards high-temperature superconductivity are highly regarded and recently reported several times in newspaper (The Nikkei), which is the most widely read in Japan, as follows ((1) July 8, 2014, The Nikkei; (2) October 19, 2013, The Nikkei; (3) November 7, 2011, The Nikkei; (4) January 14, 2011, The Nikkei; (5) November 22, 2010, The Nikkei; (6) November 18, 2010, The Nikkei).